PATTERNS OF EVOLUTIONARY DIVERSIFICATION THROUGH LINEAGES, MORPHOLOGY, AND MECHANICS

by

BARBARA LEE BANBURY

A dissertation submitted in partial fulfillment of
the requirements for the degree of

DOCTOR OF PHILOSOPHY

WASHINGTON STATE UNIVERSITY
School of Biological Sciences

May 2010

To the Faculty of Washington State University:

The members of the Committee appointed to examine the dissertation of BARBARA LEE BANBURY find it satisfactory and recommend that it be accepted.

_____
Michael E. Alfaro, Ph.D., Chair

_____
Luke J. Harmon, Ph.D.

_____
Eric Roalson, Ph.D.

_____
Michael Webster, Ph.D.

_____
Gary Thorgaard, Ph.D.

ACKNOWLEDGMENT

First, I owe a debt of personal gratitude to my academic mentors and family. In particular, my advisor Michael Alfaro, whose guidance has been a continued source of inspiration to challenge myself and excel. Also, I would like to thank my committee members for continually fomenting my professional development at many levels. In particular, Luke Harmon who has been a continual source of knowledge and assistance. Many thanks to my wonderful husband/coworker, Hugo Alamillo, for his continued emotional support, editing skills, lab assistance, and advice. Thanks to many friends and colleagues in Pullman, including members of the Harmon, Hufford and Roalson labs, for academic feedback and making Pullman a wonderful place to live. Finally, many thanks to my family for their never-ending love and support.

Second, I would like to thank those individuals that have made my research materialize. Thanks to Alissa Gildemann for her hard work in the lab for a year collecting megophryid molecular data. Thanks to David Collar and Peter Wainwright for use of the centrarchid and labrid morphological datasets, and Tom Near for use of the centrarchid chronogram. This work was supported in part by the Society for Systematic Biologists, the American Society for Ichthyologists and Herpetologists, the Society for the Study of Amphibians and Reptiles, and the National Science Foundation.

PATTERNS OF EVOLUTIONARY DIVERSIFICATION THROUGH LINEAGES, MORPHOLOGY, AND MECHANICS

Abstract

by Barbara Lee Banbury, Ph.D.
Washington State University
May 2010

Chair: Michael E. Alfaro

A fundamental challenge in evolutionary biology lies in explaining why some groups are more diverse than others. This dissertation focuses on three components of diversity: lineages, morphology, and mechanical property. The first chapter examines the relationship between morphology and mechanical property. Although morphological change is frequently interpreted as an indication of mechanical diversification it is not known whether the evolution of mechanical properties in complex traits corresponds with similar diversification patterns in underlying morphology. I focus on the feeding system of fishes that display many-to-one mapping (or functional convergence) and test whether historical patterns of mechanical and morphological evolution fit concordant models of diversification. I find that despite a tight link between the morphology and emergent mechanical properties of a trait, the diversification pattern between them can be significantly different. The second chapter focuses on ancestral state reconstruction. Many times the feature being reconstructed is not itself of interest, but rather serves as a proxy for other important (but unmeasured) characters. In this chapter, I explored the accuracy of inferring ancestral mechanical properties using simulation models and

two empirical traits. I found that precision is linked to the complexity of the mathematical model and accuracy was affected by both mathematical complexity and the number of interacting parts in the system. My results suggest caution when extrapolating mechanical property from ancestral morphology, and I argue that the same principle should be applied to many differing levels of design with hierarchical traits. Chapter three focuses on the relationship between lineage accumulation and morphological diversification in a group of "primitive" frogs (superfamily Pelobatoidea) and their most species-rich family (Megphryidae). Here, I present the first time-calibrated phylogenetic analysis of Pelobatoidea, including 52 megophryid species, using molecular data combined with fossil constraints. I also test the hypothesis that megophryids underwent an adaptive radiation using several comparative methods, including lineage-through-time plots, Monte Carlo constant rates test, disparity-through-time plots, and evolutionary likelihood model fitting. Despite their large clade size and high degree of morphological variation, we do not find the classic signature of adaptive radiation in the family Megophryidae.

TABLE OF CONTENTS

CHAPTER 3

LIST OF TABLES

LIST OF FIGURES

CHAPTER 1 page

CHAPTER 2

CHAPTER 3

CHAPTER 1

DISCORDANT EVOLUTIONARY PATTERNS OF MORPHOLOGY AND MECHANICS IN COMPLEX TRAITS

Barbara L. Banbury[1], Luke Harmon[2], and Michael E. Alfaro[3]

[1] School of Biological Sciences
Washington State University
PO Box 644236
Pullman, WA 99164-4236
Phone: 509-432-6869
Fax: 509-335-3184
bbanbury@wsu.edu

[2] Department of Biological Sciences
University of Idaho
Campus Box 443051
Moscow, ID 83844-3051
Phone: 208-885-0346
Fax: 208-885-7905
lukeh@uidaho.edu

[3] Department of Ecology and Evolutionary Biology
University of California Los Angeles
Los Angeles, CA 90095
Phone: 310-794-5019
Fax: 310-825-1978
michaelalfaro@ucla.edu

Running title: Discordant evolutionary patterns

Corresponding Author: Barbara L. Banbury

Key words: biomechanics, morphology, character evolution, disparity, likelihood modeling, diversification, many-to-one mapping

ABSTRACT

The relationship between form and function can strongly influence the evolution of biodiversity. Although morphological change is frequently interpreted as an indication of functional diversification it is not known whether the evolutionary diversification of mechanical properties in complex traits generally corresponds with similar patterns of diversification in underlying morphology. In this paper we test whether historical patterns of mechanical and morphological evolution fit concordant models of diversification in complex traits. We focus on the feeding system of fishes that display many-to-one mapping (or functional convergence). We analyze several biomechanical data sets with phylogenetic comparative methods to test whether the patterns and evolutionary models that explain trait diversity at each level are congruent. We find that despite a tight link between the morphology and emergent mechanical properties of a trait, the evolutionary pattern of diversification between them can be significantly different. In particular, uniform patterns of morphological diversification can mask patterns of mechanical diversification that are consistent with adaptive radiation or iterative adaptive radiation. Our results suggest that analysis of morphology alone may be insufficient to capture evolutionary histories of clades that are diversifying rapidly along ecological clines.

INTRODUCTION

Functional morphologists have long appreciated that changes in morphology do not necessarily produce equivalent changes in function (e.g.. Koehl, 1996). However, the evolutionary implications of the complex relationship between form and function have only recently been explored. In simple traits where morphology and mechanics are closely linked, morphological and mechanical diversity will be identical (Alfaro et al., 2004). Complexity, defined as the addition of parts or their interaction, can greatly weaken this relationship since complex traits typically have multiple combinations of morphologies that produce equivalent mechanical properties. This mechanical convergence, or many-to-one mapping, may facilitate morphological diversification by allowing morphology to evolve in the face of similar functional demands (Alfaro et al., 2004; Alfaro et al., 2005; Collar and Wainwright, 2006; Young et al., 2007; Wainwright, 2007; Strobbe et al., 2009). Previous work on systems that exhibit many-to-one mapping has shown that morphological and mechanical diversity can be partitioned unevenly across a tree (Koehl, 1996; Hulsey and Wainwright, 2002; Alfaro et al., 2004), suggesting that diversification in these levels of design can be decoupled. Furthermore, Collar and Wainwright (2006) found that rates of morphological and mechanical evolution can be significantly different from each other.

Although many hypotheses of adaptive radiation and key innovation focus on the functional importance of traits, morphology is typically used as a proxy for function in comparative analyses (Wainwright, 2007). Since many-to-one mapping weakens form-function relationships, the tempo of morphological diversity might differ significantly from the tempo of

mechanical diversity. In such cases, a strong signature of mechanical diversification along ecological axes might be obscured or completely masked by the attenuating effects morphological evolution in a convergent system. For example, the hypothesis of adaptive radiation explicitly predicts that selection on traits important for ecological function will drive evolutionary diversification (Schluter, 2000) and there are several available comparative methods to test whether trait evolution within a clade is consistent with this hypothesis (Pagel, 1999; Blomberg et al., 2003; Freckleton and Harvey, 2006; Harmon et al., in press). Furthermore, patterns of morphological diversification might suggest a rapid evolutionary radiation even when the emergent properties of functional evolution are largely similar across species.

Here we ask whether the historical pattern of mechanical diversification in complex traits has produced concordant evolutionary patterns in underlying morphology. We employ several phylogenetic comparative methods to examine the history of morphological and mechanical diversification associated with the feeding system in fishes and introduce a novel parametric statistic that explicitly tests whether the evolutionary models that explain trait diversity at each level are congruent. Furthermore we can examine standing hypotheses about adaptive or iterative radiations in these clades by examining the historical diversification. Our results suggest that in some cases, complex form-function relationships may obscure patterns of rapid ecological diversification.

MATERIALS AND METHODS

Mechanical Data Sets—We reanalyzed biomechanical data sets from two systems where many-to-one mapping of complex traits has been demonstrated. In centrarchid fishes, the suction index (SI) describes the peak morphological potential to generate negative buccal pressure and is determined by five elements (gape width, buccal length, length of the out-lever, length of the in-lever, and the epaxial cross-sectional area; see Carroll et al., 2004; Figure 1A). The mathematical relationship of morphological elements is linear, such that a unit change of an element will produce a proportional change in SI (Collar and Wainwright, 2006). Morphological measurements for 27 centrarchid species were reanalyzed from Collar and Wainwright (2006) in the context of a published time-calibrated molecular phylogeny with branch lengths in millions of years (Near et al., 2005).

Maxillary kinematic transmission (maxKT) describes the transfer of force through four bony elements connected in a loop (fixed length, nasal, maxilla, and lower jaw; Westneat, 1990; see Westneat, 1995; Figure 1B). The motion of opening the lower jaw is transmitted to the maxilla and in turn causes the upper jaw to protrude (Westneat, 1995). In this system the mathematical relationship of the underlying morphology is highly nonlinear, such that one unit change to a morphological element will have disproportionate and difficult-to-predict effects on maxKT (Muller, 1996; Hulsey and Wainwright, 2002; Alfaro et al., 2004, Alfaro et al., 2005). We completed the labrid chronogram in a separate study (Alfaro et al., 2009) and morphological measurements for maxKT (fixed length, maxilla, nasal, and lower jaw) were reanalyzed from

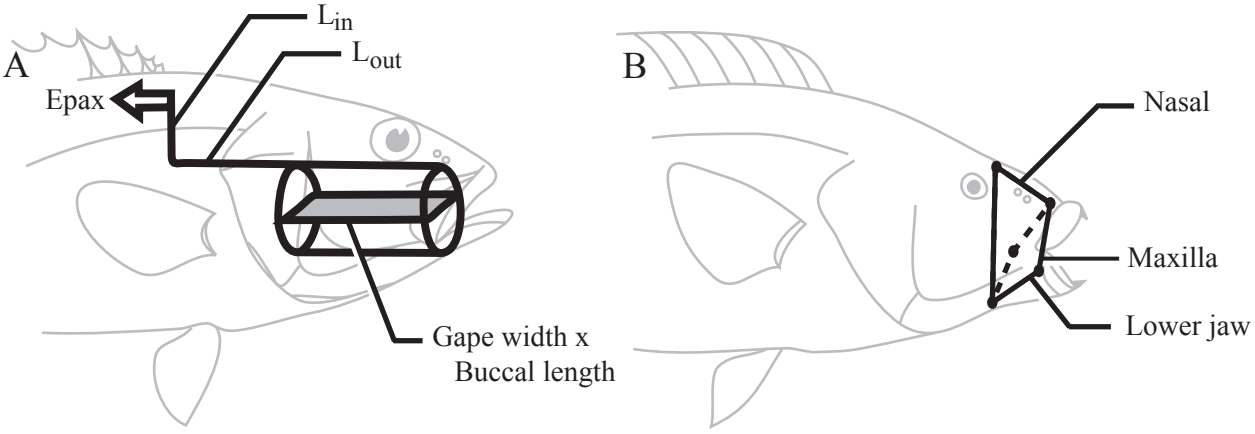

Figure. 1. (A) Diagram of the suction index of centrarchid fishes (image adapted from Collar and Wainwright, 2006). The suction index can be calculated as a ratio of the product of the epaxial muscles force (calculated as cross sectional area; Epax) and mechanical advantage (Lin × Lout) by the projected area of the buccal cavity. (B) The in jaws of labrid fish, illustrating the four-bar linkage in open position, dashed line indicates the position of the maxilla and lower jaw in a closed position (image adapted from Alfaro et al., 2005). Maxillary kinematic transmission can be calculated as the number of degrees output rotation of the maxilla (relative to the fixed link) by a given number of degrees input rotation by the lower jaw. One unit change in length of a linkage element will not have predictable change on the functional property of the mechanism; and can only be determined by knowing the geometry of the other elements.

Wainwright et al. (2004). Comparative analyses were performed on a pruned tree of 54 taxa, which was the maximum overlap between the morphological and molecular datasets.

Contrasts—One way to examine the relationship between the evolution of morphology and mechanics is to plot standardized contrasts (Felsenstein, 1985). Standardized contrasts from each morphological element were plotted against standardized contrasts from the respective mechanic and correlation coefficients were calculated. These coefficients describe the overall relationship between the change in a morphological element with its mechanic. Because these measures are not mathematically independent, we expect the correlational coefficients to be high.

Subclade Disparity—We introduce a novel test to determine if subclades within a tree are significantly diversified or constrained in their morphology or function. We first calculated subclade disparity, defined as the average pairwise Euclidean distance between species for each trait, for all clades (Foote, 1995, Foote, 1997; Fortey et al., 1996; Ciampaglio et al., 2001; Harmon et al., 2003). Standardized relative disparity was calculated by dividing each subclade disparity by the entire tree disparity. Subclades with values near zero indicate that relatively little variation is present within that clade, while values near one indicate that subclades contain much of the variation found in the whole tree. Subclade relative disparity values that are above one indicate that more variation is found in the subtree than the tree as a whole; this can happen if members of the subclade are more different, on average than random pairs in the whole tree. All disparity analyses were performed in R with the Geiger package (R Development Core Team 2006; Harmon et al., 2008).

On the basis of these subclade disparity measures we calculated a test statistic as the observed difference in morphological and mechanical disparity for a given clade. We generated a null distribution for the test statistic by simulating evolution of morphological and mechanical characters under a Brownian motion model using the optimal rate estimated on each phylogeny and calculating a null distribution for the difference in morphological and mechanical disparity for each subclade. This was a two-tailed test where differences could be either positive (larger mechanical disparity) or negative (larger morphological disparity). Significant nodes represent places in the tree that have diversified at one level of design, but remain similar at the other, which indicates subclades with the most discordant patterns of morphological and mechanical evolution.

Disparity through time—To test whether patterns of mechanical and morphological diversification were concordant across the history of the clade, we used the method of Harmon et al. (2003) to examine average relative subclade disparity through time. Low average subclade disparity indicates clades that are different from each other; this pattern is expected for clades that underwent a burst of diversification early in their history (Harmon et al., 2003). Conversely, higher than expected average relative subclade disparity indicates that clades are more convergent than expected and may indicate that subclades are repeatedly evolving to overlap in a restricted morpho- or ecospace, as has been suggested for iteratively adaptively radiating clades (Westneat et al., 2005; Cooper and Westneat, 2009). Thus we interpreted the disparity through time plots as potentially supporting three distinct evolutionary scenarios 1) Brownian motion of

character evolution (null), 2) adaptive radiation (subclade disparity lower than expected), and 3) iterative evolution (subclade disparity higher than expected).

We created disparity-through-time (DTT) plots by averaging relative disparity of each subclade for each point in time (Harmon et al., 2003). We plotted only the first two-thirds of the tree to account for uncertainty associated with missing taxa, which are likely to connect to the tree near the present day. We examined three levels of DTT: DTT of each individual morphological element, DTT of combined morphological elements, and DTT of mechanical properties. We compared these to the expected levels of morphological and mechanical disparity under a Brownian motion model of evolution by simulating the evolution of morphological characters under the optimal rate matrix given the empirical data and the phylogeny (Revell et al., 2008). We repeated this simulation 5000 times to generate a null distribution for the expected amount of subclade disparity for both traits given the phylogenies and assessed the significance between the observed and the expected distributions by comparing the area under the curve for the first two-thirds of the tree.

Evolutionary Model Fitting—As a third test of whether morphology and mechanics revealed concordant or discordant evolutionary histories, we fit explicit models of character evolution for morphology and mechanical properties to the two trait systems using AICc scores. The lower the AICc score the better the model fits the data (Akaike, 1974; Burnham and Anderson, 2002). Likelihood modeling was performed in R with the Geiger package (R Development Core Team 2006; Harmon et al., 2008). The first model we explored was Brownian motion (BM), which has a single rate parameter (σ^2) throughout the tree. This model essentially describes a continuous

character randomly walking through time, and estimates expected variation. The second model we explored was the early burst model (EB; Blomberg et al., 2003), in which σ^2 decreases with increasing time. This models increased (or burst) variation early in the tree and decreased variance in more recent branches, both of which are expected for adaptively radiating clades. Finally, we tested the fit of two random walk models with selective constraints, white noise (WN) and Ornstein-Uhlenbeck process (OU). These two models are similar in that they both model a situation where species maintain central values for their continuous characters (where α measures the strength of selection). The OU model is interesting when intermediate α is detected. A high value for α indicates that strong selection is acting on that character, whereas a lower value for α indicates that selection is less forceful. When $\alpha = 0$ the OU model reduces to the BM model (Butler and King, 2004), and as α approaches ∞ the model is equivalent to WN (Hunt, 2006). If the morphological traits and the mechanical property have evolved in a similar way, we predict to see similar model fits for each level of design. Alternatively, different model fits for the morphological and mechanical datasets would strongly suggest that many-to-one mapping of morphology could completely mask diversification in the emergent properties of complex traits.

RESULTS

Contrasts—The suction index is significantly correlated with gape size ($r = -0.55$, $p = 0.003$), but not significantly correlated with buccal length ($r = -0.37$, $p = 0.06$), the in lever ($r = 0.35$, $p =$

0.07), the out lever (r = -0.14, p = 0.49), or the epaxial muscle (r = 0.21, p = 0.29; Figure 2A–E). Kinematic transmission is significantly correlated with the length of the maxilla (r = -0.61, p = 0.0) and lower jaw (r = 0.61, p =0.0), but not significantly correlated with the length of the nasal (r =0.08 , p = 0.56; Figure 2F–H).

Subclade Disparity—Centrarchid subclades were examined for levels of relative disparity and major clades are recorded in Table 1. Several clades showed discordant patterns of mechanical and morphological evolution. *Pomoxis* et al. had high morphological disparity, but members remained mechanically similar. The *Micropterus* + *Lepomis* clade was morphologically and mechanically disparate. *Lepomis* showed similar levels of variation in both morphology and mechanical property. *Micropterus* showed very little diversification of either trait.

We found four nodes in the tree that had significantly different levels of morphological and mechanical disparity (Figure 3, Table 2). In each case morphological disparity exceeded mechanical disparity, which is concordant with the tendency for higher morphological than functional diversification in centrarchids (nodes 1–4).

Within labrids, several subclades showed extraordinary levels of disparity relative to whole tree disparity. In particular, the Hypsigenyines had a high degree of morphological variation, but an even higher degree of maxKT variation. The Scarines had high morphological disparity and relatively low functional disparity. Overall, most of the labrid clades had higher than whole-tree disparity for either morphology or maxKT. The only clade with very little variation is the Pseudochelines, which only represent two species in our dataset.

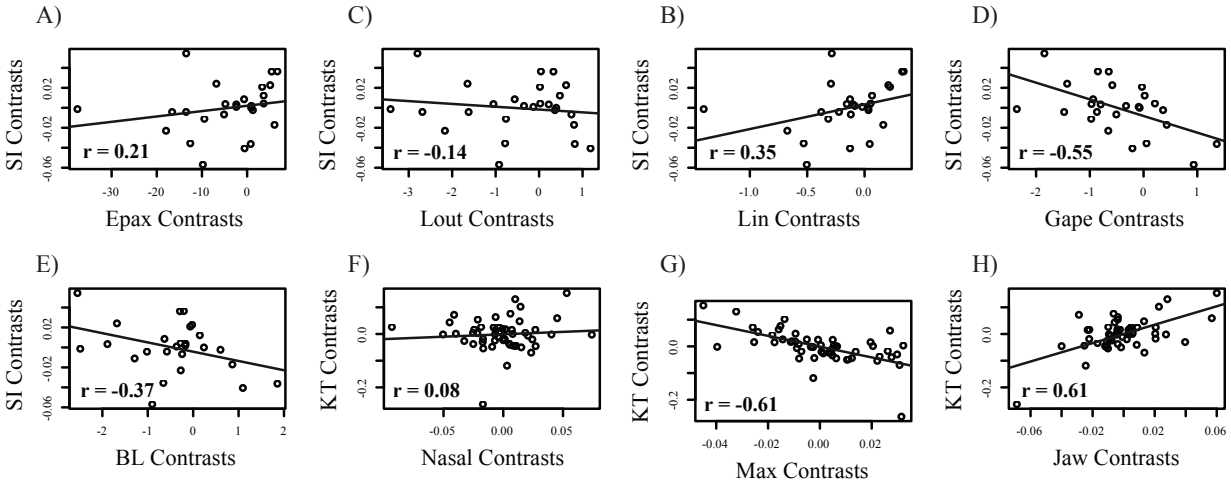

Figure 2. Plots of standardized contrasts of morphology and mechanics. (A–E) SI contrasts plotted against individual SI morphological elements; (F–H) KT contrasts plotted against individual KT morphological elements.

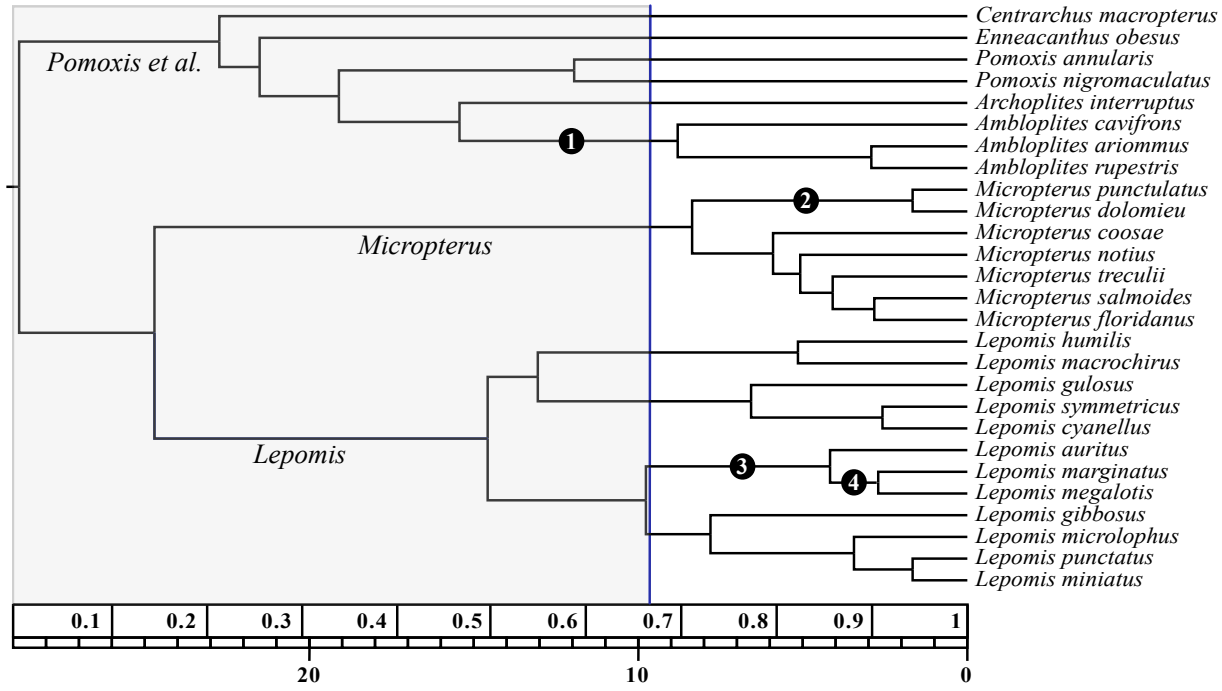

Figure. 3. Centrarchid chronogram indicating level of disparity. Nodes with morphological disparity significantly higher than functional disparity are indicated at the numbered nodes in dark circles. Timescale is shown as both millions of years (ticks at bottom) and percent of time since the origin of the clade (to correspond with disparity-through-time plots). Gray box indicates portion of the tree that was included in disparity-through-time plots as well as the measure of significance.

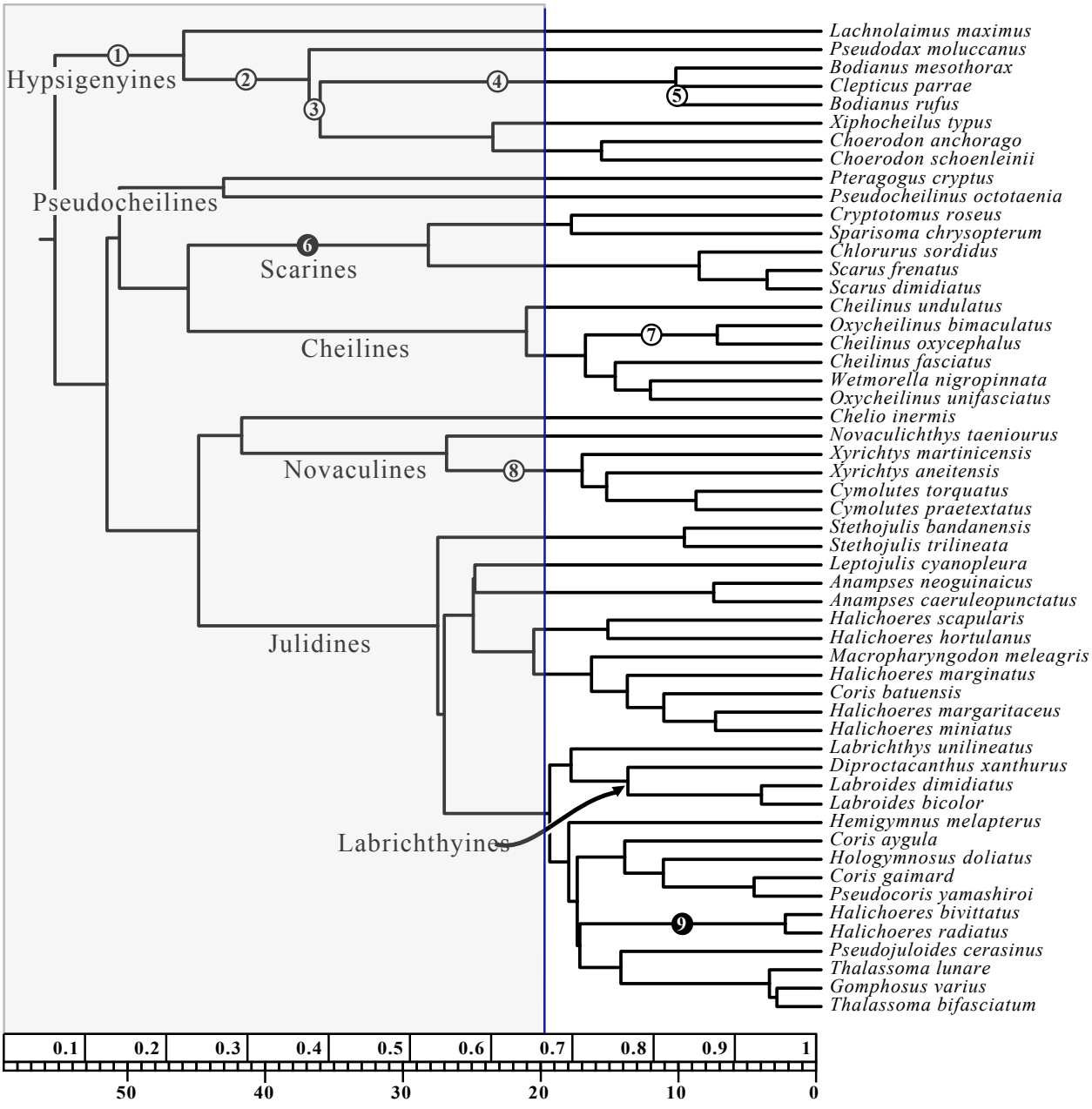

Figure. 4. Labrid chronogram indicating level of disparity. Nodes with functional disparity significantly higher than morphological disparity are indicated by numbered nodes in white circles. Nodes with morphological disparity significantly higher than functional disparity are indicated by numbered nodes in dark circles. Timescale is shown as both millions of years (ticks at bottom) and percent of time since the origin of the clade (to correspond with disparity-through-time plots). Gray box indicates portion of the tree was included in disparity-through-time plots as well as significance.

Table 1. Relative morphological and functional disparity for major subclades.

Centrarchids		
Clade	Morphology	SI
Pomoxis et al.	1.22	0.18
Micropteris + *Lepomis*	0.93	1.22
Micropteris	0.12	0.01
Lepomis	0.77	0.67
Labrids		
Clade	Morphology	maxKT
Hypsigenyines		
Non-Hypsigenyines	0.89	0.63
Pseudochelines+ Scarines + Chelines	1.05	0.43
Pseudochelines	0.09	0.00
Scarines + Chelines	1.21	0.51
Scarines	2.26	0.33
Chelines	0.40	0.65
Novaculines + Julidines + *Chelio*	0.75	0.72
Novaculines	0.44	1.37
Juladines	0.53	0.41

Table 2. Test statistics and p-values for nodes in the centrarchid and labrid trees where form and function significantly differ. These nodes reflect areas in the trees where discordance between form and function is the greatest. Positive test statistic values indicate significantly larger functional disparity, while negative numbers indicate significantly larger morphological disparity. Node numbers correspond to nodes on Figures 3 and 4.

Centrarchids		
Node	Difference	p-value
1)	-1.86	0.02
2)	-0.51	0.04
3)	-1.77	0.00
4)	-4.05	0.00
Labrids		
Node	Difference	p-value
1)	2.26	0.01
2)	2.60	0.01
3)	3.17	0.00
4)	6.07	0.00
5)	9.82	0.00
6)	-1.93	0.02
7)	1.07	0.03
8)	1.22	0.03
9)	-1.01	0.00

Several labrid subclades showed significant discordance between levels of morphological and mechanical disparity (Figure 4, Table 2). Most of the significant nodes (1–5) could be found within Hypsigenyines, which are all mechanically diverse but morphologically similar. The mechanical disparity was also significantly higher than morphological disparity at node 8 (*Xyrichtys* + *Cymolutes*). In contrast, the Scarines (node 6) were the only major subclade that is morphologically diverse but mechanically constrained. The last two significant nodes (nodes 7 and 9) might reflect a bias in the sampling. In both cases we included only two members of large clades.

Disparity through time—Average subclade disparity in centrarchids was low overall throughout the tree for the individual morphological elements, the average morphology, and the suction index (Figure 5). The individual morphological traits for the suction index were disjointed and behaved differently throughout the history of the clade. In particular, the out lever maintained the highest level of disparity throughout the clade history. For the first half of the tree, the combined morphological disparity followed the null expectation closely, was well within the confidence limits, and was not significantly different from the expectation of Brownian motion (Figure 5; $p = 0.48$). However, there was a burst of morphological disparity about 65% through the tree (~10.5 mya) that showed higher than expected diversity. Patterns of subclade disparity for the suction index were lower than expected (but not significantly lower; Figure 5; $p = 0.33$) for the first two-thirds of the tree. Within-group variation was low indicating that clades occupy isolated regions of multivariate space (Harmon et al., 2003).

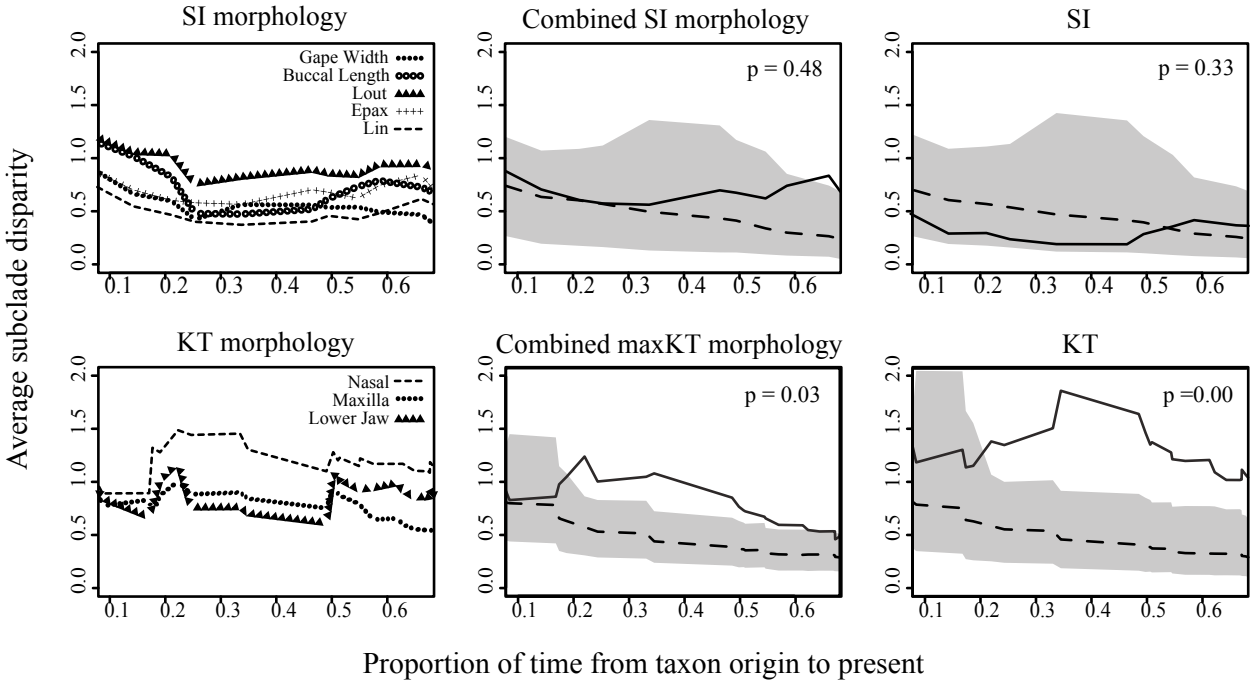

Figure 5. Disparity-through-time plots for individual morphological elements (left), combined morphology (center), and the mechanical property (right). Average disparity is calculated by averaging all ancestral subclades that were present at that given time relative to the whole-tree disparity. Time is expressed throughout the first two-thirds of the tree, because clades near the tips display greater variance among levels of disparity making the average difficult to interpret. For combined morphology and the mechanical property, average subclade disparity (solid lines) for each point in time is compared with expected disparity based on Brownian motion simulations (dashed lines with 95% confidence limits in shaded area).

Disparity through time of the individual morphological traits in labrids was even more disjunct than the centrarchids, indicating that morphological traits contribute unequal amounts to diversification of their mechanical property (Figure 5). In particular, the nasal maintains the greatest levels of disparity throughout the history of the clade. Average subclade disparity through time remained higher than expected throughout the tree for both combined morphology and maxKT and significantly deviated from the Brownian motion expectation (Figure 5; $p = 0.03$ and $p < 0.01$ respectively). Both maxKT and its morphology shared a peak of average subclade disparity around 35% through the tree (~38 mya), which is likely a reflection of the major clades of labrids (Chelines, Scarines, Novaculines, and Julidines) having diversified into their respective trophic levels. However the relative disparity within these groups remained high, indicating that subclades contain much of the disparity found in the whole tree.

Evolutionary Modeling—In the centrarchids, a Brownian motion model best fit suction index and gape width while all other morphology was best described by a random walk model with selective constraint (WN or OU) (Table 3). Buccal length, length of the out-lever, length of the in-lever, and the epaxial cross-sectional area have partitioned variation equally throughout the different ages of the tree, or are returning to a central tendency. The labrid maxillary KT and all underlying morphology was best supported by selective constraint models (WN or OU). Neither mechanical property nor underlying morphology was best supported by the early burst model, which is one model for rapid diversification expected during an adaptive radiation.

Table 3. AICc scores from four models of evolution: Brownian motion (BM), early burst (EB), white noise (WN), and Ornstein-Uhlenbeck (OU) for each function and its respective morphology (all values were log transformed). AICc scores presented do not take into account measurement error and numbers in bold represent the best-fit model. Likelihood modeling that incorporates measurement error was also tested for fit, there were no differences in best-fit models when error was ≤ 0.05.

	BM	EB	WN	OU
SI	**-54.84**	-52.27	-34.02	-53.42
Gape Width	**141.33**	143.90	150.97	142.21
Buccal Length	148.89	151.45	**144.29**	146.04
Epaxial CSA	350.02	352.59	419.57	**265.68**
In Lever	93.40	95.97	90.82	**88.31**
Out Lever	159.56	162.13	**145.45**	148.02
	BM	EB	WN	OU
maxKT	31.68	33.94	**8.36**	9.57
Nasal	-76.19	-73.94	**-90.37**	-88.17
Maxilla	-111.18	-108.93	-102.94	**-114.31**
Lower Jaw	-97.85	-95.60	**-108.87**	-107.59

DISCUSSION

Our analyses revealed that although the mechanical properties of SI and maxKT are exactly determined by morphology, the inferred evolutionary pattern of diversification between these levels are different. Despite several significant correlations of standardized contrasts, the general pattern showed a large amount of incongruence. Furthermore, we found that variation in form is not partitioned the same across either phylogeny as variation in function. In the case of the labrids, both morphology and maxKT maintained high relative subclade disparity throughout the tree indicating repeated character turnover and character convergence. However, the signal for convergence is much stronger in maxKT than in morphology. This suggests that labrid history is characterized by subclades that strongly overlap in the mechanical property of their oral jaws even though the underlying morphology is diverse. In contrast, analysis of diversification patterns within centrarchids revealed patterns of functional convergence that are weaker than the underlying morphology suggests. Below we consider the implications of our analyses for each subclade and for the understanding of the evolutionary diversification of complex traits in other systems.

Diversification of suction index and maxKT—Centrarchids are an ecologically diverse clade of freshwater fish that display multiple trophic strategies (Lauder, 1983; Huckins, 1997; Collar et al., 2009). Despite this, previous authors have demonstrated functional constraint and slow character turnover (Collar et al., 2006; Collar et al., 2009). Our evolutionary analysis is consistent with these ideas; we find low diversity within major groups and higher diversity

between groups. Although our results are not statistically significant, this pattern is consistent with initial diversification into differing trophic strategies and limitations on diversification within those trophic niches.

From the disparity analyses we find that centrarchids show greater diversification in morphology than in function. Although neither pattern differed significantly from expectations under a Brownian model of evolution, this disparity is maintained throughout most of the early history of centrarchids. This corroborates results from the relative disparity of the major centrarchid subclades that have low subclade disparity within and high disparity between major groups. The highest subclade disparity for suction index is the *Micropterus* + *Lepomis* clade (Table 1), but there is small diversity found within each of these genera. This pattern indicates that diversification occurred early in centrarchid history. Variation is partitioned among the groups rather than within, which suggests that initial diversification occurred into different mechanical and morphological spaces and since then has been maintained.

The low variation in the suction index for the genera *Pomoxis* et al. and *Micropterus* may be attributed to mechanical constraint or stabilizing selection (Collar and Wainwright, 2006). The genus *Micropterus* has especially low subclade disparity for both morphology and mechanical property. This is consistent with the idea that these fish have limited diversification due to their high functional demands to maintain piscivory (Collar et al., 2009). However *Pomoxis* et al. has relatively high degree of morphological diversity, which is consistent with the hypothesis that many-to-one mapping can undergo morphological diversification while remaining functionally neutral (Alfaro et al., 2004; Alfaro et al., 2005; Collar and Wainwright,

2006; Wainwright, 2007). This diversification could stem from selection on the morphology from other ecological pressures or simply be a result from phenotypic drift.

Previous studies have suggested that labrids have repeatedly converged in functional space on the basis of high homoplasy in functional characters (Alfaro et al., 2004; Westneat et al., 2005). Our study provides quantitative support for repeated rapid character turnover throughout the tree and a high degree of functional convergence within subclades.

Labrids show high levels of relative disparity throughout their history indicating subclades contain much of the variation found in the whole tree. The highest peak in disparity for both morphology and function is 40–50% of time since their origin (29–36 mya) is likely a reflection of the diversification between the major clades of labrids (Chelines, Scarines, Novaculines, and Julidines). Westneat et al. (2005) found that each labrid subclade contained overlapping ecological strategy for maxKT demonstrating a high degree of functional convergence and/or reversal of states. We find similar results using disparity in that many of the subclades contain relative disparity values near or higher than one indicating clades have evolved to overlap in morphological space (Harmon et al., 2003). This rapid character turnover could easily explain the high diversity we see among these groups and supports the idea that labrids have had iterative adaptive radiations into differing trophic levels (Westneat, 1995; Westneat and Alfaro, 2005; Cooper and Westneat, 2009).

The results from the evolutionary likelihood modeling analysis are in good agreement with results from our disparity analyses. The suction index and gape width both fit the Brownian motion model the best, as both SI and gape width show decreased variation among closely related taxa. This pattern is largely concordant with patterns we observe in the disparity-

through-time analysis (see Figure 5). The other morphological traits within the suction index fit a more parameter-rich model best (either WN or OU) that model the trait returning to a central value.

Evolutionary model fitting of maxKT and its morphology all fit the more parameter rich models. No trait fit the early burst model, which would support labrids as a single adaptive radiation, but this makes sense in light of our disparity results. If the labrids are displaying an iterative adaptive radiation in their subclades we would not expect the early burst model to fit for the entire tree. Instead these traits return to a central value, indicating that species stay in an ideal region of mechanical- or morphological space regardless to the amount of time that has passed.

Conclusions—The tempo of morphological diversification can be strongly incongruent with the pattern of mechanical diversification. Mechanical diversification does not produce similar signatures in the underlying morphology. Although morphology is often used as a proxy for mechanical or ecological diversification, our results suggest that this practice could lead to an inference that is at odds with the true character history. Therefore, comparative studies of complex traits that use morphology as a substitute for mechanical properties might be misleading. Even the evolution of individual morphological elements within a mechanical system are incongruent, possibly because they co-function in seperate mechanical traits or are correlated with other morphological traits.

Our results strongly argue for the inclusion of ecologically relevant mechanical measures in comparative studies, as patterns of diversification could be missed if only morphology is

examined. While patterns of morphological diversification are intrinsically interesting, caution must be used when interpreting the morphological patterns as indicators of mechanical or ecological diversification.

LITERATURE CITED

Akaike, H. 1974. A new look at the statistical model identification. IEEE Trans. Automat. Contrl. 19:716–723.

Alfaro, M. E., D. I. Bolnick, and P. C. Wainwright. 2004. Evolutionary dynamics of complex biomechanics: an example using the four-bar mechanism. Evolution 58:495–503.

Alfaro, M. E., D. I. Bolnick, and P. C. Wainwright. 2005. Evolutionary consequences of many-to-one mapping of jaw morphology to mechanics in labrid fishes. American Naturalist 165(6):140–154.

Alfaro M.E., C. Brock, B.L. Banbury, and P. Wainwright. 2009. Does evolutionary innovation in pharyngeal jaws lead to adaptive radiation? Evidence from analysis of diversification in labrids and parrotfishes. BMC Evolutionary Biology 9:255.

Blomberg S. P., T. Garland, and A. R. Ives. 2003. Testing for phylogenetic signal in comparative data: Behavioral traits are more labile. Evolution 57(4):717–745.

Burnham, K. P., and D. R. Anderson. 2002. Model selection and multimodel inference: a practical information-theoretic approach. 2nd Edition. Springer-Verlag, New York, New York, USA. 488 pp.

Butler, M. A., and A. A. King. 2004. Phylogenetic comparative analysis: a modeling approach for adaptive evolution. Am. Nat. 164:683–695.

Carroll, A. M., P. C. Wainwright, S. H. Huskey, D. C. Collar, and R. G. Turingan. 2004. Morphology predicts suction feeding performance in centrarchid fishes. J. Exp. Biol. 207:3873–3881.

Ciampaglio, C. N., M. Kemp, and D. W. McShea. 2001. Detecting changes in morphospace occupation patterns in the fossil record: characterization and analysis of measures of disparity. Paleobiology 27:695–715.

Collar, D. C., and P. C. Wainwright. 2006. Discordance between morphological and mechanical diversity in the feeding mechanism of centrarchid fishes. Evolution 60(12):2575–2584.

Collar, D. C., P. C. Wainwright, and M. E. Alfaro. 2008. Integrated diversification of locomotion and feeding in labrid fishes. Biology Letters 4(1):84–86.

Collar, D. C., B. C. O'Meara, P. C. Wainwright, T. J. Near. 2009. Piscivory limits diversification of feeding morphology in centrarchid fishes. Evolution 63(6):1557–1573.

Cooper, W. J., and M . W. Westneat. 2009. Form and function of damselfish skulls: rapid and repeated evolution into a limited number of trophic niches. BMC Evolutionary Biology 9:24.

Felsenstein, J. 1985. Phylogenies and the comparative method. American Naturalist. 125:1–15.

Foote, M. 1995. Morphological diversification of Paleozoic crinoids. Paleobiology 21:273–299.

Foote, M. 1997. The evolution of morphological disparity. Annual Review of Ecology and Systematics 28:129–158.

Fortey, R. A., D. E. G. Briggs, and M. A. Wills. 1996. The Cambrian evolutionary 'explosion': Decoupling cladogenesis from morphological disparity. Biol. J. Linn. Soc. 57(13):13–33.

Freckleton, R. P. and P. H. Harvey. 2006. Detecting non-Brownian trait evolution in adaptive radiations. PLoS 4(11):2104–2111.

Harmon, L. J, J. A. Schulte II, A. Larson, and J. B. Losos. 2003. Tempo and mode of evolutionary radiation in iguanian lizards. Science 301: 961–964.

Harmon, L. J., J. T. Weir, C. D. Brock, R. E. Glor, and W. Challenger. 2008. GEIGER: investigating evolutionary radiations. Bioinformatics 24(1):129–131.

Harmon, L. J., J. B. Losos, J. Davies, R. G. Gillespie, J. L. Gittleman, W. B. Jennings, K. Kozak, M. A. McPeek, F. Moreno-Roark, T. J. Near, A. Purvis, R. E. Ricklefs, D. Schluter, J. A. Schulte II, O. Seehausen, B. Sidlauskas, O. Torres-Carvajal, J. T. Weir, & A. Ø. Mooers. In press. Body size and shape rarely evolve in early bursts.

Huckins, C. J. F. 1997. Functional linkages among morphology, feeding performance, diet, and competitive ability in molluscivorous sunfish. Ecology 78(8):2401–2414.

Hulsey, C. D., and P. C. Wainwright. 2002. Projecting mechanics into morphospace: disparity in the feeding system of labrid fishes. Proc. R. Soc. Lond. B 269:317–326.

Hunt, G. 2006. Fitting and comparing models of phyletic evolution: random walks and beyond. Paleobiology 32:578–601.

Koehl, M. A. R. 1996. When does morphology matter? Annu. Rev. Ecol. Syst. 27:501–542.

Lauder, G. V. Functional and morphological bases of trophic specialization in sunfishes (Teleostei, Centrarchidae). Journal of Morphology 178(1):1–21.

Muller, M. 1996. A novel classification of planar four-bar linkages and its application to the mechanical analysis of animal systems. Philos. Trans. R. Soc. Lond. B Biol. Sci. 351:689–720.

Near, T. J., D. I. Bolnick, and P. C. Wainwright. 2005. Fossil calibrations and molecular divergence time estimates in centrarchid fishes (Teleostei: Centrarchidae). Evolution 59:1768–1782.

Pagel, M. 1999. Inferring the historical patterns of biological evolution. Nature 401:877–884.

R Development Core Team. 2006. R: A language and environment for statistical computing. R Foundation for Statistical Computing, Vienna, Austria. ISBN 3-900051-07-0, URL http://www.R-project.org.

Revell, L. J., L. J. Harmon, and D. C. Collar. 2008. Phylogenetic signal, evolutionary process, and rate. Syst. Biol. 57(4):591–601.

Schluter, D. 2000. The ecology of adaptive radiation. Oxford University Press, Oxford.

Strobbe, F., M. A. McPeek, M. De Block, L. De Meester, and R. Stoks. 2009. Survival selection on escape performance and its underlying phenotypic traits: a case of many-to-one mapping. J. Evol. Biol. 22:1172–1182.

Wainwright, P. C. 2007. Functional versus morphological diversity in macroevolution. Annu. Rev. Ecol. Evol. Syst. 38:381–401.

Wainwright, P. C., D. R. Bellwood, M. W. Westneat, J. R. Grubich, and A. S. Hoey. 2004. A functional morphospace for the skull of labrid fishes: patterns of diversity in a complex biomechanical system. Biological Journal of the Linnean Society 82:1–25.

Wainwright, P. C., A. M. Carroll, D. C. Collar, S. W. Day, T. E. Higham, and R. A. Holzman. 2007. Suction feeding mechanics, performance, and diversity in fishes. Integrative and Comparative Biology 47(1):96–106.

Westneat, M. W. 1990. Feeding mechanics of teleost fishes (Labridae): a test of four-bar linkage models. Journal of Morphology 205:269–295.

Westneat, M. W. 1995. Feeding, function, and phylogeny: analysis of historical biomechanics in labrid fishes using comparative methods. Systematic Biology 44:361–383.

Westneat, M. W. and M. E. Alfaro. 2005. Phylogenetic relationships and evolutionary history of the reef fish family Labridae. Molecular Phylogenetics and Evolution 36(2):370–390.

Westneat, M. W., M. E. Alfaro, P. C. Wainwright, D. R. Bellwood, J. R. Grubich, J. L. Fessler, K. D. Clements, and L. L. Smith. 2005. Local phylogenetic divergence and global evolutionary convergence of skull function in reef fishes of the family Labridae. Proc. R. Soc. 272:993–1000.

Young, R. L., T.S. Haselkorn, and A.V. Badyaev. 2007. Functional equivalence of morphologies enables morphological and ecological diversity. Evolution 61: 2480–2492.

CHAPTER 2

ACCURACY OF ANCESTRAL STATE RECONSTRUCTION IN COMPLEX TRAITS

Barbara L. Banbury[1], Luke Harmon[2], and Michael E. Alfaro[3]

[1] School of Biological Sciences
Washington State University
PO Box 644236
Pullman, WA 99164-4236
Phone: 509-432-6869
Fax: 509-335-3184
bbanbury@wsu.edu

[2] Department of Biological Sciences
University of Idaho
Campus Box 443051
Moscow, ID 83844-3051
Phone: 208-885-0346
Fax: 208-885-7905
lukeh@uidaho.edu

[3] Department of Ecology and Evolutionary Biology
University of California Los Angeles
Los Angeles, CA 90095
Phone: 310-794-5019
Fax: 310-825-1978
michaelalfaro@ucla.edu

Running title: Accuracy of ancestral state reconstruction in complex traits

Corresponding Author: Barbara L. Banbury

Key words: biomechanics, many-to-one mapping, morphology, ancestral state reconstruction, complex traits, functional morphology

ABSTRACT

Reconstructing ancestral states is a common method in comparative biology. However many times the feature being reconstructed is not itself of interest, but rather serves as a proxy for other more important (but unmeasured) characters. In this paper we focused on inferring ancestral biomechanical property from reconstructed ancestral morphology. We explored the accuracy of inferring ancestral mechanical properties using simulation models. We compare both hypothetical traits of varying complexity and two empirical traits under a well-understood biomechanical model. We compared both precision and accuracy for two scenarios for reconstructing ancestral states of mechanical property: 1) we reconstructed ancestral morphology from terminal morphology using ancestral state reconstruction and solved for ancestral mechanical property, or 2) we estimated ancestral mechanical property from known terminal mechanical property using ancestral state reconstruction. We found that precision is linked to the complexity of the mathematical model. Estimates of mechanical property are less precise in more complex models. Accuracy was affected by both the complexity of the mathematical model and the number of interacting parts in the system. Our results suggest caution when extrapolating mechanical property from ancestral morphology, and we argue that the same principle should be applied to many differing levels of design with hierarchical traits.

Key words: biomechanics, morphology, character evolution, ancestral state reconstruction, many-to-one mapping

INTRODUCTION

Reconstructing ancestral states is a common and useful method in comparative biology for determining past evolutionary events. Many methods have been proposed to estimate ancestral states for both discrete (e.g. Ronquist, 1996; Pagel, 1999; Pagel and Meade, 2006; Minin and Suchard, 2008) and continuous (e.g. Felsenstein, 1981; Maddison, 1991; Schluter et al., 1997; Martins, 1999) characters given various optimality criteria. However many times the feature being reconstructed is not itself of interest, but rather serves as a proxy for other more important (but unmeasured) characters. For example, one might wish to reconstruct individual nucleotides in a DNA sequence and use them to infer the ancestral function of the gene (e.g. Yang et al., 1995; Liberles, 1997; Krishnan et al., 2004). These hierarchical character inferences are made at many different levels of design, and yet we know little to nothing about their statistical properties. This paper focuses on one aspect of hierarchical inference: the accuracy and precision of inferring ancestral function from ancestral morphology.

Morphological features are routinely used to infer biomechanical, functional, or ecological properties. Ideally, the relationship between form and mechanical properties can be described by a mathematical equation, which can range from simple to highly complex. In the simplest cases, trait morphology relates directly to trait property in a one-to-one relationship. This one-to-one relationship means that there is only a single morphology corresponding to any particular biomechanic, and evolving towards that mechanical property results in predictable morphological changes. One example is a simple lever system (e.g. the lower jaw of fish; Barel, 1977). As a result of this one-to-one mapping, species with mechanically similar traits will have

similar underlying morphology (Bouton et al., 2002; Lovette et al., 2002; Alfaro et al., 2004). Inferences between form and mechanics in these cases seem straightforward.

If there are three or more morphological parts in the system carrying out a single function, there will be multiple combinations of morphology that produce equivalent mechanical properties (Wainwright, 2007). This mechanical redundancy (or many-to-one mapping, *sensu* Alfaro et al., 2004) means that species with similar mechanics can have drastically different underlying morphology (Hulsey and Wainwright, 2002; Alfaro et al., 2004; Alfaro et al., 2005; Wainwright et al., 2005; Wainwright, 2007). This extinguishes the possibility of inferring morphology from mechanics. Even if one can unilaterally solve for the mechanical property when the morphology is known, it is not possible to reconstruct individual values of morphology from the emergent biomechanical property.

Thus increasing the "complexity" of a system weakens the relationship between morphology and mechanics. This complexity can arise from two factors. One factor that may increase complexity in the system is the number of morphological parts in the system (Alfaro et al., 2004). As morphological elements are added there will be more possible combinations that produce equivalent functions (Alfaro et al., 2004; Wainwright et al., 2007). The second factor contributing to complexity is the mathematical relationship between parts in the system (Koehl, 1996, Alfaro et al., 2004). As the relationship of underlying morphological elements strays from linearity, changes in any given element may have dramatic effects on the emergent property. This weakens the correlation between the amount of morphological and functional diversification across species (Alfaro et al., 2004; Banbury et al., in review).

In this paper, we examined the degree of mathematical error when inferring complex hierarchical

traits from underlying traits using morphology-mechanic relationships as our model. We used a variety of theoretical traits that differed in the number of parts and complexity of the mathematical model between morphology and mechanics. We also used models from two case studies where biomechanical properties are well understood. We assessed both the accuracy of inferred ancestral states compared to known values, and precision by comparing estimates of ancestral mechanical property across two scenarios: 1) ancestral mechanics was estimated from known tip mechanical property using ancestral state reconstruction, and 2) ancestral morphology was estimated from tip morphology using ancestral state reconstruction and put into a model to calculate ancestral mechanical property. If precision is high, the two methods should converge on the same estimate.

MATERIALS AND METHODS

Simulated Datasets

We carried out simulations in R with the Geiger package (R Development Core Team, 2006; Harmon et al., 2008). First, we simulated a 50-taxon pure-birth tree (b=1, d=0). Then we evolved morphological characters across the tree according to Brownian motion using the identity matrix as an evolutionary variance-covariance matrix (so that all traits had a net rate of evolution $\sigma^2 = 1$, and there were no expected covariances among traits). For most simulations we set the root state at zero, allowing character change in both positive and negative ranges.

From the simulated terminal morphology, we applied several mathematical formulae relating morphology to mechanics in varying degrees of complexity. The simplest model we

examined was a strictly additive model where the theoretical mechanic (*f*) was equal to the sum of the morphological traits (m_i; Eqn. 1). This model was applied over a varying number of traits.

$$f = \sum_{i=2}^{100} (m_i) \tag{1}$$

Second, we examined the effect of functional properties determined as a ratio (Eqn. 2). In this model, we set the number of morphological traits constant (at n = 4). To explore the effect of varying amounts of nonlinearity in the model we varied the expected mean of these characters at the tips of the tree by using different root (ancestral) states equal to 0, 5, and 10. Functional values can change dramatically under this model when morphological character values are near zero.

$$f = \frac{m_1 + m_2}{m_3 + m_4} \tag{2}$$

Third, we examined several multiplicative models with two, three, four, and six morphological traits (Eqn 3).

$$f = \prod_{i=2}^{6} (m_i) \tag{3}$$

Next, we explored a combination of additive and multiplicative models with four, six, and eight morphological traits with two, three, and four multiplicative terms respectively (Eqn. 4).

$$f = \sum_{i=1,j=1}^{3} (m_i m_j) \tag{4}$$

Lastly, we explored the use of the sine function into an additive and multiplicative model using just two morphological traits (Eqns. 5 and 6).

$$f = \sum_{i=2} \sin(m_i) \tag{5}$$

$$f = \prod_{i=2} \sin(m_i) \tag{6}$$

To get an adequate degree of variation among trees and morphology, each mathematical model was simulated 300 times. We then used terminal character states for calculations of terminal functions and for ancestral state reconstruction. The character states of internal nodes were recorded so that reconstructed mechanical values could be compared with the actual ancestral mechanical values.

Case Studies

We also examined the behavior of two actual measures of feeding performance from teleost fishes: the suction index (SI; Carroll et al., 2004) for the family Centrarchidae and maxillary kinematic transmission (maxKT; Westneat, 1990; Westneat, 1995) for the family

Labridae. Since both traits involve feeding they are likely to have strong fitness consequences for individuals in the wild. Additionally, both systems have multiple arrangements of morphological traits that produce equivalent emergent properties (many-to-one mapping; Stadler et al., 2001; Hulsey and Wainwright, 2002; Alfaro et al., 2004, 2005; Collar and Wainwright, 2006). These two biomechanical traits are particularly attractive to study because both the morphology-mechanic relationship and the phylogenetic relationships within each group are well understood. Given this, we can apply ancestral state reconstruction methods to reconstruct both morphology and mechanical property and determine if discord between the two methods exists.

Our SI dataset was reanalyzed from Collar et al. (2006) on centrarchid fishes. A total of 27 species have information regarding SI and SI morphology (gape width, buccal length, length of the out-lever, length of the in-lever, and the epaxial cross-sectional area). These traits were examined across a well-resolved time-calibrated phylogeny for centrarchids (Near et al., 2005). Our maxKT dataset, including maxKT and maxKT morphology (fixed length, maxilla, nasal, and lower jaw), were reanalyzed from Wainwright et al. (2004). Comparative analyses were performed on a pruned tree of 54 taxa (Alfaro et al., 2009), which was the maximum overlap between the morphological and molecular datasets.

Ancestral State Reconstruction Methods

For all simulated datasets, ancestral states for individual morphological elements and their respective mechanics were reconstructed using maximum likelihood under a Brownian motion model in the Geiger package in R (R Development Core Team, 2006; Harmon et al., 2008). These ancestral estimates are exactly equivalent to ancestral states estimated under

weighted squared-change parsimony (Schluter et al., 1997; Webster and Purvis, 2002).

We calculated ancestral mechanical property two ways. First, ancestral mechanical property ($\hat{f}_j$) was estimated directly from the known tip mechanics (f_j), where *j* represents a node (ancestral or extant; herein Method 1). Ancestral mechanical property was calculated a second way, by estimating ancestral morphology ($\hat{m}_{i,j}$) from the known tip morphology ($m_{i,j}$), where *i* represents a morphological trait and *j* represents a node (ancestral or extant; herein Method 2). The estimated ancestral morphology at internal nodes was placed into its respective equation, and estimated ancestral mechanical property ($\hat{\phi}_j$) was calculated. See Figure 1 for an example.

Measuring precision and accuracy

We evaluated both the accuracy and the precision of the two methods for inferring ancestral function described above. Accuracy was assessed by comparing the two estimates of ancestral mechanical property ($\hat{f}_j$ and $\hat{\phi}_j$) to the real ancestral mechanic that was stored from the simulation. For this part of the study, we tracked two nodes in the simulated trees: 1) the root node, and 2) the most recent node (varies from simulation to simulation). For each tracked node, we measured the difference between the real vale and the estimated value. Summary statistics were calculated from 300 simulations within a model. To assess precision, we compared estimates of ancestral mechanical property ($\hat{f}_j$ and $\hat{\phi}_j$) for each internal node of the tree using

Pearson product-moment correlation. If the two values are similar throughout the tree, then reconstructing ancestral morphology is robust to particular methodological decisions about how to assess ancestral function. In this scenario, we expect the Pearson product-moment correlation coefficient (r) to be close to 1.0. However, if the order of reconstructing ancestral mechanics matters, we expect a low correlation between our two methods for predicting ancestral mechanics.

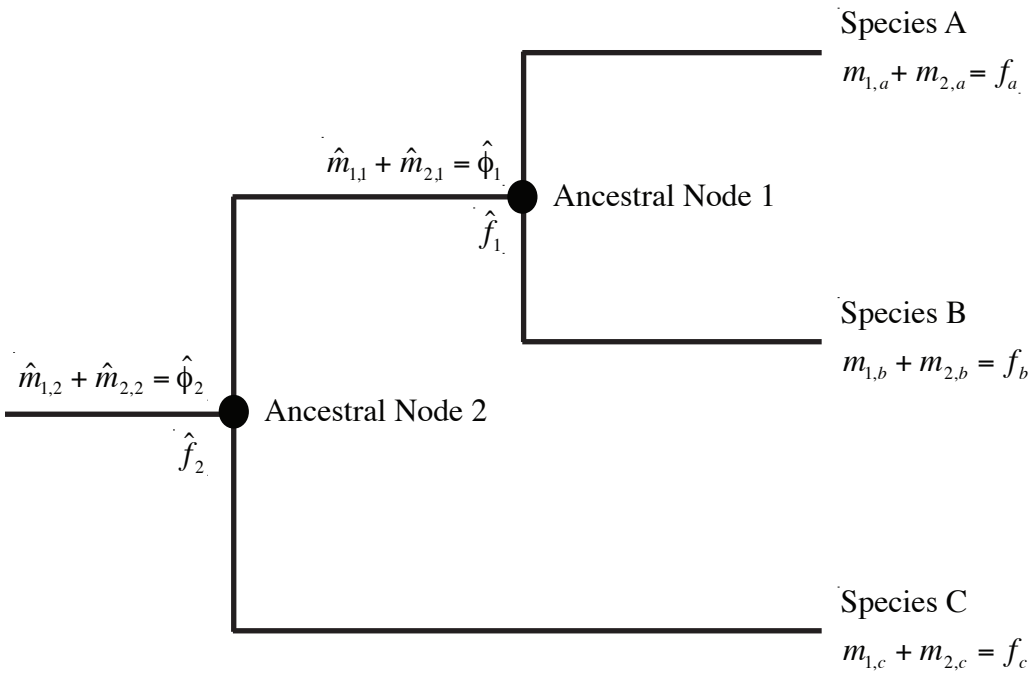

Figure 1. Hypothetical state illustrating the two methods we used to calculate ancestral mechanics. The first method estimated ancestral function ($\hat{f}_j$) from tip function (f_j) using one-parameter maximum likelihood (Method 1), and the second method estimated ancestral morphology ($\hat{m}_{i,j}$) from tip morphology ($m_{i,j}$) using one-parameter maximum likelihood and placed into a functional model to calculate ancestral function ($\hat{\phi}_j$; Method 2). In all cases *i* represents a morphometric trait and *j* represents a node (ancestral or extant).

RESULTS

Simulations

Accuracy.—We calculated the difference between the estimates from each method of mechanical reconstruction ($\hat{f}_j$'s and $\hat{\phi}_j$'s) with the actual ancestral values from simulations. These differences were pooled and standard deviations were calculated (Table 1). Each model had error associated with ancestral reconstruction, however none of the models show substantial over- or underestimation bias.

The accuracy of reconstruction under an additive model tends to decrease as the number of parts in the system increase (Eqn. 1; Table 1; Figure 2A–B). There was no difference in accuracy between reconstruction methods, which was expected as the models were 100% precise. The mathematical models that incorporated a ratio had high accuracy when the tip values were positive (linear relationship; Eqn. 2; Table 1), but had very low accuracy when the root state was set at 0 so that tip values were both positive and negative (Table 1). The accuracy of the reconstruction under a multiplicative model (Eqn. 3) also decreases with increasing complexity (Table 1; Figure 2C–D).

Table 1. Standard deviations for the difference between estimated and actual ancestral states across mathematical models. $SD_{\hat{f}_j}$ = Method 1, $SD_{\hat{\phi}_j}$ = Method 2.

Eqn.	Model	n	Root State	Most Recent Node		Root Node	
				$SD_{\hat{f}_j}$	$SD_{\hat{\phi}_j}$	$SD_{\hat{f}_j}$	$SD_{\hat{\phi}_j}$
1)	$f = \sum_{i=2}^{100}(m_i)$	2	0	1.74	1.74	1.46	1.46
		4	0	2.01	2.01	2.27	2.27
		8	0	3.83	3.83	2.89	2.89
		100	0	16.56	16.56	10.68	10.68
2)	$f = \frac{m_1 + m_2}{m_3 + m_4}$	4	10	0.09	0.09	0.10	0.09
		4	5	0.35	0.33	0.39	0.23
		4	0	14.26	24.29	45.82	80.35
3)	$f = \prod_{i=2}^{6}(m_i)$	2	0	2.67	2.68	1.48	1.04
		3	0	4.77	4.64	3.43	2.14
		4	0	8.07	7.22	4.18	1.85
		6	0	78.99	71.83	16.27	4.19
4)	$f = \sum_{i=1,j=1}^{3}(m_i m_j)$	4	0	2.98	2.92	2.37	1.59
		6	0	3.79	3.67	2.57	1.94
		8	0	4.60	4.52	3.67	2.60
5)	$f = \sum_{i=2}\sin(m_i)$	2	0	0.80	0.82	0.33	0.82
		2	10	0.79	0.84	0.35	0.78
6)	$f = \prod_{i=2}\sin(m_i)$	2	0	0.49	0.56	0.12	0.39
		2	10	0.45	0.50	0.14	0.44

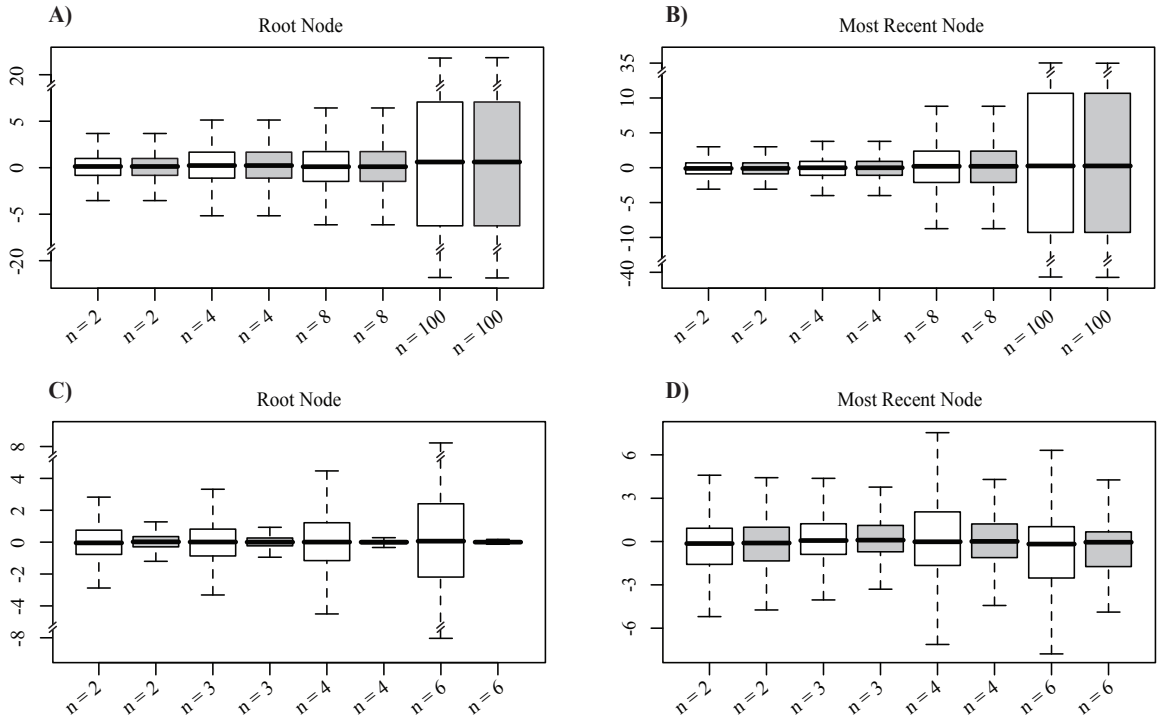

Figure 2. Boxplot graphs indicating the difference between the estimated ancestral value and the actual ancestral value for additive models (A–B) and multiplicative models (C–D). Ancestral estimates from Method 1 (using tip function) are shown as white boxes, whereas estimates of ancestral mechanic from Method 2 (using tip morphology) are shown with shaded boxes. Black bars indicate the mean, boxes are for the upper and lower quantiles, 95% of the data falls within the error bars. n = number of morphological traits in the model.

We compared the results from the multiplicative models to the results from the additive plus multiplicative models (Eqn. 4; Table 1) that increase the number of parts to the system, but do not increase the degree of the equation. In this case, we saw a decrease in accuracy as the number of parts increases, but not to the same degree as the multiplicative models, indicating that model complexity is the predominant factor for decreasing accuracy. A second pattern emerged from the multiplicative and additive plus multiplicative models: reconstructed ancestral values using tip function ($\hat{f}_j$) have higher standard deviation than reconstructed values from tip morphology ($\hat{\phi}_j$) and are therefore less accurate. The trigonometric models had fairly high accuracy (Eqn. 5–6; Table 1). Neither the root state nor the methodology had an effect on accuracy.

Precision.— From the pooled correlations of $\hat{f}_j$'s and $\hat{\phi}_j$'s we calculated the mean and standard deviation of r-values for each mathematical model tested. These summary statistics are presented in Table 2. All additive models were perfectly correlated (Eqn. 1; $\bar{x} = 1$, SD = 0.0; Fig. 3A), regardless of the number of morphological traits included in the system. The models that include ratios (Eqn. 2) had varying precision based on the root state. When the root state was large (and thus terminal morphology was also large), the correlation between reconstructed ancestral mechanics was high ($\bar{x}$ = 0.99, SD = 0.002; Fig. 3B). However as terminal morphology decreased in value, we found increasing differences between the two estimates of ancestral function. When terminal morphology spanned zero precision was dramatically reduced ($\bar{x}$ = 0.09, SD = 0.31).

Table 2. Mean and standard deviation r-values from precision analyses of theoretical datasets, where n equals the number of morphological traits included in the model.

Eqn	Model	n	Root State	$\bar{x}$	SD
1)	$f = \sum_{i=2}^{100}(m_i)$	2	0	0	0
		4	0	0	0
		8	0	0	0
		100	0	0	0
2)	$f = \frac{m_1 + m_2}{m_3 + m_4}$	4	10	0.99	0.002
		4	5	0.98	0.03
		4	0	0.09	0.31
3)	$f = \prod_{i=2}^{6}(m_i)$	2	0	0.92	0.07
		3	0	0.83	0.14
		4	0	0.74	0.20
		6	0	0.59	0.28
4)	$f = \sum_{i=1,j=1}^{3}(m_i m_j)$	4	0	0.92	0.07
		6	0	0.92	0.06
		8	0	0.92	0.07
5)	$f = \sum_{i=2}\sin(m_i)$	2	0	0.82	0.12
		2	10	0.82	0.13
6)	$f = \prod_{i=2}\sin(m_i)$	2	0	0.67	0.18
		2	10	0.65	0.17

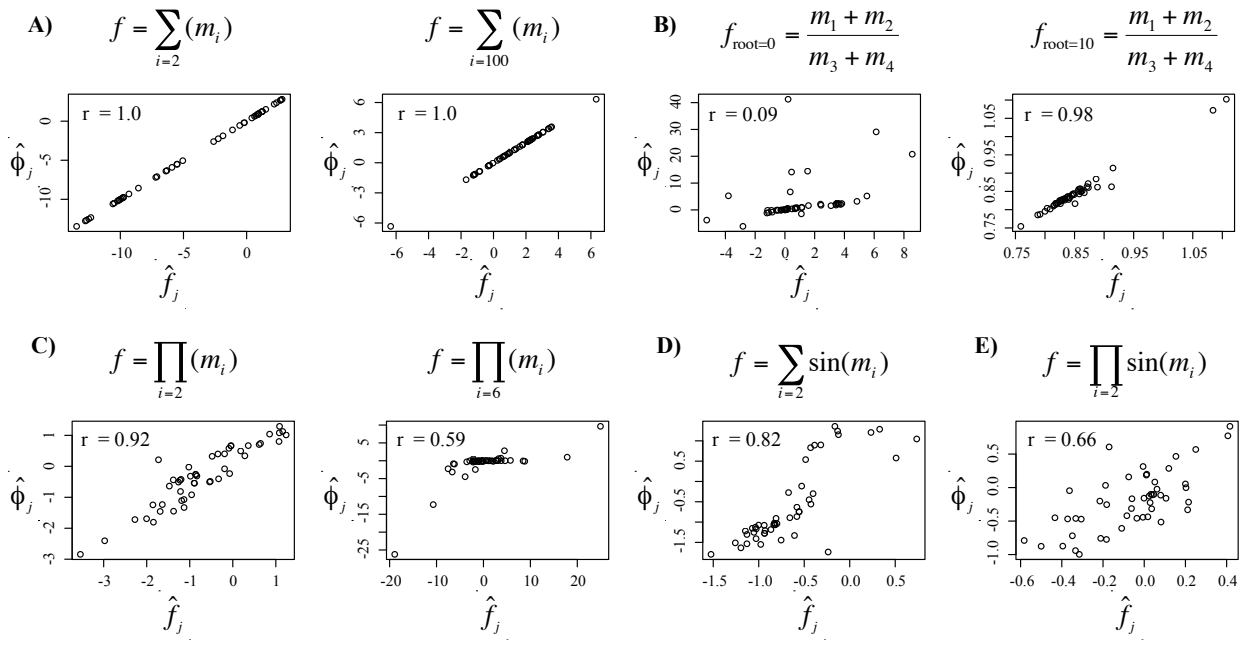

Figure 3. Selected linear regressions from precision analyses of theoretical traits with an r-value close to the mean of all simulations. Estimated ancestral mechanics from tip function ($\hat{f}_j$) are on the x-axis and estimated ancestral mechanics from the morphology ($\hat{\phi}_j$) are on the y-axis. n = number of morphological traits in the model.

The multiplicative models (Eqn. 3) showed decreased mean correlation coefficients and increased variation between reconstructed ancestral mechanics as the degree of the equation increased ($\bar{x}$ = 0.92–0.59, SD = 0.07–0.28; Fig. 2C). Interestingly, the additive plus multiplicative models (Eqn. 4) did not show the same pattern. In these equations, the initial decrease in correlation stemmed from a single multiplicative term, and adding multiplicative terms did not decrease precision further ($\bar{x}$ = 0.92, SD = 0.06–0.07).

The trigonometric models we examined (Eqns. 5–6) also showed a reduction in precision when compared with their similar non-trigonometric counterparts ($\bar{x}$ = 0.82, SD = 0.12–0.13 and $\bar{x}$ = 0.67–0.65, SD = 0.17–0.18, respectively; Fig. 2D–E). However, neither of the trigonometric models changed in precision when we changed the root state.

Case Studies

The estimated ancestral mechanics ($\hat{f}_j$ and $\hat{\phi}_j$) for suction index had a strong relationship (r = 0.99; Fig. 4A), and thus high precision between the two methods for reconstructing ancestral mechanics. Conversely, the two estimates for ancestral maxillary KT had a fairly weak relationship and included some strong outliers (r = 0.67; Fig. 4B). For maxKT, precision between the two methods is weak, and thus choice in methodology is important. Furthermore, there were some combinations of ancestral maxKT morphology that could not produce an ancestral value for maxKT (mathematically impossible based on the fit of the morphology). These data points had to be discarded from the correlation analysis, making the correlation coefficient an overestimate of the fit between the two methods of reconstruction.

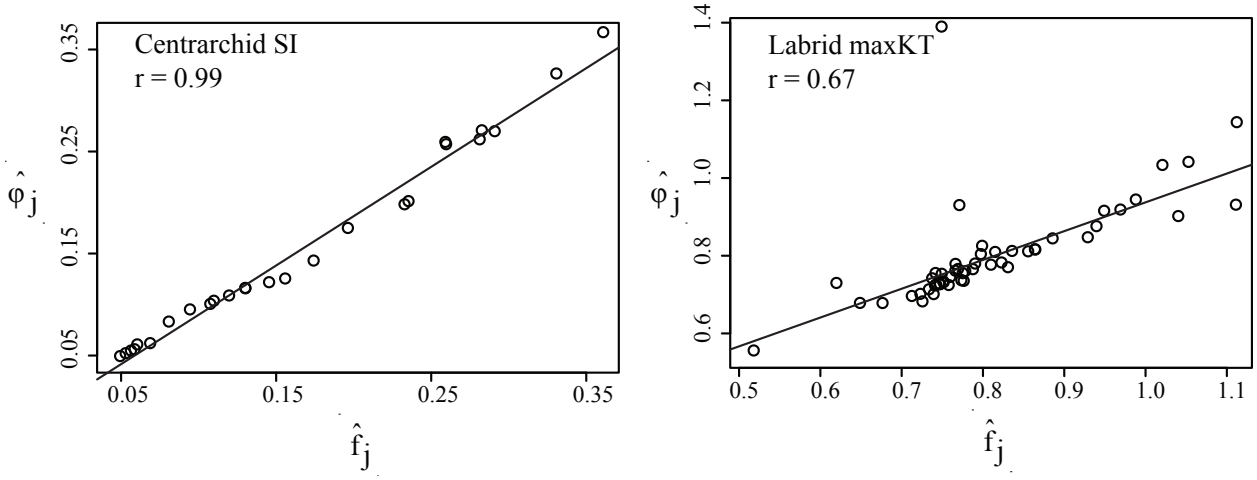

Figure 4. Correlation of the estimates of ancestral mechanics ($\hat{f}_j$ and $\hat{\phi}_j$) from (A) centrarchid suction index (B) labrid maxillary KT.

DISCUSSION

We determined both the accuracy and precision of two methods of reconstructing ancestral mechanics under a variety of mathematical models. Because there were no confounding effects from biological error in our simulations (such as phylogenetic uncertainty, missing taxa, selection on traits, etc), we were able to focus solely on the mathematical error associated with inferring ancestral mechanics from ancestral morphology under different mathematical models. By definition, if *accuracy* is high the method does a good job of estimating ancestral mechanics. We compared accuracy results across mathematical models and methods of reconstruction and three generalities emerged: 1) there was more error associated with tipward nodes than root nodes, 2) error increased as both number of elements in the system increased and as complexity of the model increased, and 3) Method 1, reconstructing ancestral function from tip function, tended to have higher error than Method 2. If *precision* is high, then methodological choice is not important as either method will converge on the same ancestral estimate. However, our results suggested that precision decreases as the mathematical relationship of underlying morphology becomes more complex. Interestingly, we also found that precision and accuracy are not necessarily linked. We found some models to be highly precise and not accurate, and vice versa.

Case Studies

Both the centrarchid and labrid systems have highly integrated morphology working together to create an emergent mechanic. However the underlying morphology interacts very

differently in these two systems. The suction index, which is additive when log transformed, interacts in a predictable manner with changes to morphology resulting in proportional changes to SI. Thus we expected to see results from the correlation analysis that were similar to the simulation results from the additive models. Our observed results supported this idea; we saw a tight correlation between the two estimates of ancestral suction index, i.e. from morphology and from function (Figure 4A). This also indicates that ancestral state reconstruction of the suction index is robust to the method of reconstruction.

Maxillary kinematic transmission interacts nonlinearly to its underlying morphology, resulting in unpredictable changes when morphology is altered. We expected to see results similar to other nonlinear models that we simulated, such as the multiplicative models. Again we found what we expected, the precision between the two methods of reconstruction is low. The two estimates of ancestral maxKT were not only lacking in precision, but they also had a skewed relationship (Figure 4B). This indicates that either one method of reconstruction consistently underestimates ancestral values or the other method overestimates ancestral values. Furthermore, there were values of ancestral morphology that reconstructed values of maxKT outside of its working range. Clearly this system is sensitive to the method of ancestral state reconstruction.

Which method of estimating ancestral function is the most accurate?

Despite being many-to-one, the estimated ancestral mechanics from the additive models we explored were in perfect agreement regardless of the number of morphological elements (see Figure 3A–B). Although estimates were not perfectly accurate for either the root node or the

most recent node, accuracy decreased as the number of parts in the system increased (Figure 2A). Accuracy also decreases with an increasing number of parts, because each reconstruction comes with a small amount of error; however, precision between the two estimates is unaffected by this property. In this situation, the two methods will give identical ancestral estimates, both will be equally precise, and equally inaccurate.

In every other model we tested there was a difference in the accuracy between methodologies, although on average we converge on the correct ancestral state (ie, no skewed bias) individual estimates were inaccurate. We found that Method 2 (estimating ancestral mechanics from tip morphology) had less variance and therefore outperformed Method 1 (estimating ancestral mechanics from tip mechanics; Figure 2), which was expected given that we simulated morphology across the tree. Had we simulated the evolution of function across the tree, we would expect to see higher accuracy in estimating ancestral function from tip function. This relationship between evolution and methodological accuracy in simulated datasets is likely how real biological systems work as well.

In real datasets, differences between the real ancestral value and either estimate likely depends on the course of evolution for those traits. Ancestral taxa may have been exposed to selective pressures and/or biological constraint, both of which will affect the evolution of the morphological-mechanic relationship. Because many-to-one mapping can facilitate diversification at either level of design, morphology and mechanical property may be evolving under different evolutionary models (Banbury et al., in review). Thus, the accuracy of ancestral state reconstruction methodologies likely depends on the evolutionary processes of the system;

whichever method is closer to the model that generated the diversification will have higher accuracy.

Conclusions

We found that accuracy and precision of reconstructing ancestral states in complex morphology-mechanic relationships is affected by the complexity of the mathematical model. The results of this paper urge caution when extrapolating ancestral mechanics from ancestral form. Although we focused on morphology-mechanic relationships, we believe that this should be applied to many differing levels of design. Many-to-one mapping not only occurs between form-function relationships, but at all other pertinent biological levels.

LITERATURE CITED

Alfaro, M. E., D. I. Bolnick, and P. C. Wainwright. 2004. Evolutionary dynamics of complex biomechanics: an example using the four-bar mechanism. Evolution 58:495–503.

Alfaro, M. E., D. I. Bolnick, and P. C. Wainwright. 2005. Evolutionary consequences of many-to-one mapping of jaw morphology to mechanics in labrid fishes. American Naturalist 165(6):140–154.

Alfaro M.E., C. Brock, B.L. Banbury, and P. C. Wainwright. 2009. Does evolutionary innovation in pharyngeal jaws lead to adaptive radiation? Evidence from analysis of diversification in labrids and parrotfishes. BMC Evolutionary Biology 9:255.

Banbury B.L., L. Harmon, and M.E. Alfaro. In review. Discordant evolutionary patterns of morphology and mechanics in complex traits. Journal of Evolutionary Biology.

Barel, C. D. N. 1977. Kinematischer Transmissionskoeffizient und Vierstangensystem als Funktionsparameter und Formmodel fur Mandibulare Depressionsapparate bei Teleostiern. Ann. Anat. 142:21–31.

Bouton, N., J. De Visser, and J. Barel. 2002. Correlating head shape with ecological variables in rock-dwelling haplochromines (Teleostei: Cichlidae) from Lake Victoria. Biol. J. Linn. Soc. 76:39–48.

Carroll, A. M., P. C. Wainwright, S. H. Huskey, D. C. Collar, and R. G. Turingan. 2004. Morphology predicts suction feeding performance in centrarchid fishes. J. Exp. Biol. 207:3873–3881.

Collar, D. C., and P. C. Wainwright. 2006. Discordance between morphological and mechanical diversity in the feeding mechanism of centrarchid fishes. Evolution 60(12):2575–2584.

Felsenstein J. 1981. Evolutionary trees from gene frequencies and quantitative characters—finding maximum likelihood estimates. Evolution 35:1229–1242.

Harmon, L. J., J. T. Weir, C. D. Brock, R. E. Glor, and W. Challenger. 2008. GEIGER: investigating evolutionary radiations. Bioinformatics 24(1):129–131.

Hulsey, C. D., and P. C. Wainwright. 2002. Projecting mechanics into morphospace: disparity in the feeding system of labrid fishes. Proc. R. Soc. Lond. B 269:317–326.

Koehl, M. A. R. 1996. When does morphology matter? Annu. Rev. Ecol. Syst. 27:501–542.

Krishnan, N.M. H. Selegmann, C. B. Stewart, A. P. De Koning, and D. D. Pollock. 2004. Ancestral sequence reconstruction in primate mitochondrial DNA: compositional bias and effect on functional inference. Molecular Biology and Evolution 21 (10):1871–1883

Liberles, D. A. (ed.). 2007. Ancestral sequence reconstruction. Oxford University Press, New York.

Lovette, I. J., E. Bermingham, and R. E. Ricklefs. 2002. Clade specific morphological diversification and adaptive radiation in Hawaiian songbirds. Proc. R. Soc. Lond. B Biol. Sci. 269:37–42.

Maddison, W. P. 1991. Squared-change parsimony reconstructions of ancestral states for continuous-valued characters on a phylogenetic tree. Systematic Zoology 40:304–314.

Martins, E. P. 1999. Estimation of ancestral states of continuous characters: a computer simulation study. Systematic Biology 48:642–650.

Minin, V. N., and M. A. Suchard. 2008. Fast, accurate and simulation-free stochastic mapping. Philosophical transactions of the Royal Society B 636(1512):3985–3995.

Near, T. J., D. I. Bolnick, and P. C. Wainwright. 2005. Fossil calibrations and molecular divergence time estimates in centrarchid fishes (Teleostei: Centrarchidae). Evolution 59:1768–1782.

Pagel, M., and A. Meade. 2006. Bayesian analysis of correlated evolution of discrete characters by reversible-jump Markov chain Monte Carlo. American Naturalist 167(6):808–825.

Pagel, M. 1999. The maximum likelihood approach to reconstructing ancestral character states of discrete characters on phylogenies. Systematic Biology 48(3):612–622.

R Development Core Team. 2006. R: A language and environment for statistical computing. R Foundation for Statistical Computing, Vienna, Austria. ISBN 3-900051-07-0, URL http://www.R-project.org.

Ronquist, F. 1995. Reconstructing the history of host-parasite associations using generalised parsimony. Cladistics 11:73–90.

Schluter, D., T. Price, A. O. Mooers, and D. Ludwig. 1997. Likelihood of ancestor states in adaptive radiation. Evolution 51:1699–1711.

Stadler, B. M. R., P. F. Stadler, G. P. Wagner, and W. Fontana. 2001. The topology of the possible: formal spaces underlying patterns of evolutionary change. Journal of Theoretical Biology 213:241–274.

Wainwright, P. C., D. R. Bellwood, M. W. Westneat, J. R. Grubich, and A. S. Hoey. 2004. A functional morphospace for the skull of labrid fishes: patterns of diversity in a complex biomechanical system. Biological Journal of the Linnean Society 82:1–25.

Wainwright, P. C., M. Alfaro, D. I. Bolnick and C. D. Hulsey. 2005. Many-to-one mapping of form to function: a general principle in organismal design? Integrative and Comparative Biology 45(2):256–262.

Wainwright, P. C. 2007. Functional versus morphological diversity in macroevolution. Annu. Rev. Ecol. Evol. Syst. 38:381–401.

Wainwright, P. C., A. M. Carroll, D. C. Collar, S. W. Day, T. E. Higham, and R. A. Holzman. 2007. Suction feeding mechanics, performance, and diversity in fishes. Integrative and Comparative Biology 47(1):96–106.

Webster, A. J., and A. Purvis. 2002. Testing the accuracy of methods for reconstructing ancestral states of continuous characters. Proceedings of the Royal Society B 269:143–149.

Westneat, M. W. 1990. Feeding mechanics of teleost fishes (Labridae): a test of four-bar linkage models. Journal of Morphology 205:269–295.

Westneat, M. W. 1995. Feeding, Function, and Phylogeny: Analysis of Historical Biomechanics in Labrid Fishes Using Comparative Methods. Systematic Biology 44:361–383.

Yang, Z., S. Kumar, and M. Nei. 1995. A new method of inference of ancestral nucleotide and amino acid sequences. Genetics 141 (4):1641–1650.

CHAPTER 3

LINEAGE ACCUMULATION AND MORPHOLOGICAL DIVERSIFICATION OF THE SUPERFAMILY PELOBATOIDEA (ANURA: ARCHAEOBATRACHIA)

Barbara L. Banbury[1]

[1] School of Biological Sciences
Washington State University
PO Box 644236
Pullman, WA 99164-4236
Phone: 509-432-6869
Fax: 509-335-3184
bbanbury@wsu.edu

Key words: Megophryidae, Pelobatoidea, diversification, LTT, DTT, character evolution, adaptive radiation

ABSTRACT

The superfamily Pelobatoidea is a large group of "primitive" frogs (suborder Archaeobatrachia) consisting of four families (Pelobatidae, Pelodytidae, Scaphiopodidae, and Megophryidae). The most species rich family within the superfamily is the family Megophryidae that consists of approximately 140 species in ten genera. Aside from being the most successful family within Pelobatoidea by species numbers, the family Megophryidae also displays incredible morphological and ecological diversity. The central goals of this work is to propose the first large-scale phylogeny for the superfamily Pelobatoidea, begin interpreting the evolutionary diversification of lineages and morphology, and explicitly test whether the family Megophryidae underwent an adaptive radiation. We present the first time-calibrated phylogenetic analysis of the superfamily Pelobatoidea, including a large number of megophryid species, using molecular data combined with fossil constraints. We test the hypothesis that the megophryids underwent an adaptive radiation using several comparitive methods, including lineage-through-time plots (LTT), Monte Carlo constant rates test (MCCR), disparity-through-time plots (DTT), and evolutionary likelihood model fitting. Despite their large clade size and high degree of morphological variation, we do not find the classic signature of adaptive radiation in the family Megophryidae.

INTRODUCTION

The superfamily Pelobatoidea is a large group of "primitive" frogs (suborder Archaeobatrachia) with a near-global distribution. It consists of four families (Pelobatidae, Pelodytidae, Scaphiopodidae, and Megophryidae). Although the phylogenetic relationships within and among Pelobatoidea has a long contentious history, most recent molecular phylogenies that use statistical approaches based on molecular data agree that the group is monophyletic (García-Paris et al., 2003; Dubois, 2005; Frost et al., 2006; Roelants et al., 2007; Wiens, 2007) and contains these four distinct lineages.

The family Pelobatidae is a single genus (*Pelobates*; 4 species) with an Old World distribution through Europe, western Asia, and northwestern Africa. These species are predominately fossorial and have interesting adaptations to desert life, including modified spade-like digits for burrowing, hyperossified crania, and reduced larval periods. They share many characteristics with the family Scaphiopodidae, a New World family comprised of two genera (*Scaphiopus* and *Spea*; 3 and 4 species respectively). Morphological evidence typically unites these two families, however molecular evidence does not support this (García-Paris et al., 2003; Dubois, 2005; Frost et al., 2006; Roelants et al., 2007; Wiens, 2007). Instead, it seems their morphological similarities are due to extensive homoplasy given their extreme desert lifestyles.

The family Pelodytidae includes a single genus (*Pelodytes*; 3 species) from southwestern Europe. Unlike their spadefoot relatives (families Pelobatidae and Scaphiopodidae), these frogs are average-looking smooth-skinned pond frogs. They do not bear the same modifications for desert survival, but are thought to be most closely related to scaphiopodids (García-Paris et al.,

2003; Dubois, 2005; Frost et al., 2006; Roelants et al., 2007; Wiens, 2007).

The most species rich family in the superfamily Pelobatoidea is the family Megophryidae that consists of approximately 140 species in ten genera (*Borneophrys*, *Brachytarsophrys*, *Leptobrachella*, *Leptobrachium*, *Leptolalax*, *Megophrys*, *Ophryophryne*, *Oreolalax*, *Scutiger*, *Xenophrys*). Aside from being the most successful family within Pelobatoidea by species numbers, the Family Megophryidae also displays incredible morphological and ecological diversity. Most are small (about 20–160 mm) ground dwelling frogs from south and Southeast Asia with a broad North-South distribution from temperate deciduous forest to tropical rainforest. In addition, they occur at an extensive range of altitudes and have been collected everywhere from sea level to the slopes of the Himalayas at 5100 meters. Despite the extensive range of habitats, many species require old-growth forests with dense canopies that can provide ample leaf litter. Many species have cryptic coloration and epidermal structures that resemble parts of leaves, which allow them to camouflage.

The family Megophryidae: A compelling case of adaptive radiation?

Adaptive radiations are thought to lead to increased rates in both trait diversification and species diversity (Schluter, 2000). Clades that we consider to have adaptively radiated, such as African Lake Cichlids or Caribbean Anoles (e.g. Losos and Miles, 2002), are both morphologically diverse and species rich. One objective when studying adaptively radiating clades is to identify events that triggered a radiation or factors that might predispose a clade to radiate (e.g. Lovette et al., 2002; Nosil and Crespi, 2006; Mangel et al., 2007). These factors can be either extrinsic (e.g. ecological opportunity) or intrinsic (e.g. key innovation). However,

morphological diversity and species richness are not always linked. Several studies demonstrated that morphological diversification can be decoupled from lineage diversification, such that some lineages can be species rich and morphologically depauperate (e.g. *Albinaria* snails, Gittenberger, 1991; and plethodontid salamanders, Kozak et al., 2006) or species poor and morphologically diverse (e.g. pygopodid lizards, Webb and Shine, 1994).

Until recently, studies of adaptive radiations were largely qualitative, as no quantitative criteria existed to recognize clades that had undergone unusually great divergence from clades that exhibit the normal degree of adaptive variation. Losos and Miles (2002) put forth a set of criteria that would distinguish morphologically diverse clades from others. They also suggested that disparity, a measure of character distance between species, is a suitable metric for quantifying differences in variation. Harmon et al. (2003) expanded these methods and compared ecomorphological disparity with patterns of cladogenesis. Their results indicated that clades whose lineage diversification occurred disproportionately early in their evolutionary history partitioned morphological disparity among (rather than within) subclades, which is consistent with the idea of adaptive radiation involving both species and morphological diversity.

Because the family Megophryidae displays exceptional diversity compared to other Archaeobatrachian clades, it is possible the family underwent a adaptive radiation. Several recent large-scale studies on anuran diversification identified the megophryid clade as having experienced higher than average rates of lineage diversification (Roelants et al., 2007; Wiens, 2007). However, little is known about the tempo or mode of this diversification.

Many questions still remain unanswered for megophryid systematics. Some progress has

been made at the generic level (Brown et al., 2009), however a higher-level phylogenetic analysis for the family that shows relationships of major groups and tests monophyly (and taxonomic validity) of traditionally recognized groups has not been presented. Here we present the first time-calibrated phylogenetic analysis of the superfamily Pelobatoidea, including a large number of megophryid species, using molecular data combined with fossil constraints. The central goals of this work are to propose the first large-scale phylogeny for the superfamily Pelobatoidea, begin interpreting the evolutionary diversification of lineages and morphology, and explicitly test whether the family Megophryidae underwent an adaptive radiation.

MATERIALS AND METHODS

Molecular Data Collection and Analysis

DNA sequence data for 75 frogs was examined in this study, including 13 outgroup taxa (*Ascaphus*, three discoglossids, four bombinatorids, and five pipids) and 62 pelobatoid taxa, 52 of which are megophryid taxa. All specimens were obtained through museum gifts and most have voucher specimens associated with the tissue. Twenty-four sequences (mostly outgroup taxa) were downloaded from GenBank to augment novel sequences generated from this study.

Genomic DNA was isolated from liver or muscle tissues preserved in 95% ethanol using Chelex protocol (Bio-Rad). Aliquots of the supernatant were retained for template DNA for polymerase chain reaction (PCR). Double-stranded DNA products from two mitochondrial genes (12S rDNA and 16S rDNA) were amplified. Each 25 µl PCR reaction contained 1–2 µl

DNA template (20–50 ng/µl), 5.0 µl 10X reaction buffer (Roche, Mannheim, Germany), 2.0 µl $MgCl_2$, 0.5 µl premixed deoxynucleic triphosphates (8 µM) , 0.125 µl *Taq* polymerase (Roche, Mannheim, Germany), and 1.25 µl of each oligonucleotide primer (10 µM). Primers used for amplification and sequencing were the same as Graybeal (1997).

Each PCR included an initial denaturation step at 94 ºC for 3 minutes, followed by 40 cycles of PCR (denaturation at 94 ºC for 30 seconds, annealing at 49–55 ºC for 105 seconds, and extension at 72 ºC for 60 seconds), and a final extension step at 72 ºC for 5 minutes. Successful PCR products were cycle-sequenced at the Yale DNA Analysis Facility using a 96-capillary Genetic Analyzer (Applied Biosystems, Foster City, CA).

Sequences from both genes were edited and contigs of overlapping regions were created using Sequencher 4.8 (Gene Codes). Initial sequence alignments were constructed using Muscle v3.7 (Edgar, 2004), and finalized by eye using the visual alignment editor Se-Al (Rambaut, 1996). Sequences for both genes were trimmed to the shortest sequence to minimize the amount of missing data in phylogenetic analyses. Ambiguously alignable regions for ribosomal subunits (identified by eye) usually correspond with hypervariable loop regions and were excluded from the analyses. After trimming sequence ends and the ambiguously alignable regions, the 12S gene contained 1006 base pairs and the 16S gene contained 599 base pairs.

Morphological Sampling

Morphology was examined for 110 pelobatoid species (n = 1287) including 99 megophryid species (n = 1154), using calipers and a dissecting scope to measure morphological traits of adult specimens. Standard morphometric measurements for traits that spanned feeding, locomotor, and sexual systems were collected. The following seventeen measurements were

examined for each individual: snout-vent length (SVL), pelvic width, pectoral width, head length, and head width for general measurements of body size; intraocular distance, eye height, tympanic height, and tympanic width for prey capture and predator avoidance; iliac length, femoral length, tibiafibular length, calcaneus-astragalis length, and foot length as measures of jumping performance; and humeral length, radioulnar length, and hand length as measures of locomotion, maneuverability, and display.

Divergence Time Estimation

Divergence times and tree topology were simultaneously estimated under a relaxed clock using Baysian MCMC (BEAST, Drummond and Rambaut, 2003; Drummond et al., 2006). Two nodes were constrained in the analysis based on the archaeobatrachian fossil record. In both cases, the estimated age of the fossil set a hard bound on the minimum age of the clade. The maximum age of the clade was set as a soft bound, and represented a best estimate given external information (for example, the age of an anuran fossil can not be older than the age of anurans). The minimum and maximum dates were incorporated into exponential priors to mitigate the effects of truncation (Yang and Rannala, 2006; Rannala and Yang, 2007), where the 95% upper limit reflected the maximum date set for the fossil.

1) Crown Pipoidea— (Figure 1, Node 1) The fossil *Cordicephalus gracilis* from the Lower Cretaceous was used as a crown group estimate for the minimum age of pipoids (*Rhinophrynus* + Pipidae; 121 MY; Trueb and Bàez, 2006). The maximum age was set at 280 MY to reflect the first appearance of anurans (Roelants et al., 2007).

2) Crown Scaphiopodidae—(Figure 1, Node 2) The fossil *Scaphiopus guntheri* (previously included within North American "*Eopelobates*") from the Middle Eocene is the earliest known North American scaphiopodid (49 MY; Henrici, 2000). This fossil provides a minimum estimate for the age of the stem group *Scaphiopus*. An upper bound of the crown *Scaphiopus* was placed at 155 MY to reflect the unlikeliness of *Scaphiopus* being older than the crown group Pelobatoidea (Garcìa-Paris et al., 2003).

Two independent repeats of BEAST MCMC were run to 100 million generations and sampled every 1000 generations. Convergence was assessed visually using Tracer (Rambaut and Drummond, 2007) and AWTY (Wilgenbusch et al., 2004), by examination of likelihood scores versus generation and estimates of effective sample size (ESS).

Lineage accumulation

Several phylogenetic comparative methods were applied with the chronogram to test hypotheses regarding the patterns of species diversification. All diversification statistics were performed using source code implemented in R (R Development Core Team, 2006).

To test for a constant rate of cladogenesis through time, the CR test was applied to calculate the γ statistic (Pybus and Harvey, 2000). Incomplete taxon sampling may lead the CR test to infer declining rates of cladogenesis through time erroneously, because of uncaptured nodes at the tree's tips (Pybus and Harvey, 2000). To correct for this, 1000 Monte Carlo simulations of tree topologies were created based on a Yule process of speciation (pure birth) to create a null distribution for the γ statistic (MCCR test; Pybus and Harvey, 2000). Because of

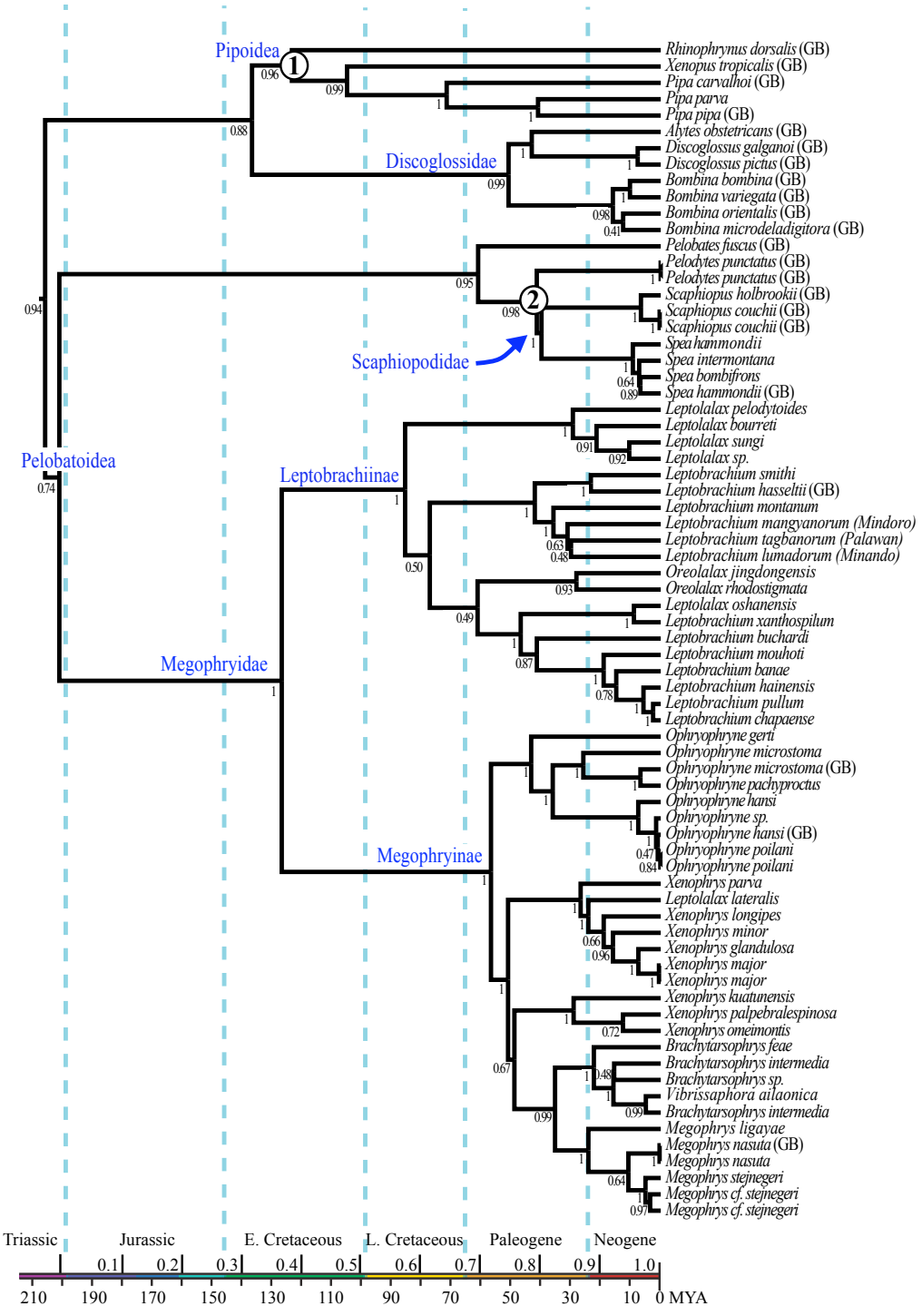

Figure 1. Time-calibrated phylogeny (chronogram) of pelobatoid frogs. Numbered circles correspond with fossil-calibrated nodes. Posterior probability is indicated under each node. Species with (GB) indicate that their sequence data was downloaded from Genbank. Numbers under the timeline represent actual ages, while numbers above the line indicate proportion of the clade history (consistent with disparity analyses)

the effect of the pull of the present, we can only assess whether rates have significantly decreased throughout the history of the clade (one-tailed test).

Lineage accumulation through time was investigated using lineage-through-time plots (LTT Plots; Nee et al., 1992) for the superfamily Pelobatoidea and the family Megophryidae. The LTT plot compares the actual number of lineages that have accumulated throughout a clades history to a null expectation simulated under a Yule (pure birth) model through simulations. These simulations incorporate missing taxa, by randomly pruning out the same number of taxa that are missing from the dataset. Using these plots, an accelerated rate of diversification early in megophryid history was tested (indication of early radiation) by calculating the area between the two plots generated under the null and observed plots for the first third of the tree (Alfaro et al., 2007; Alfaro et al., 2008).

Morphological diversification

To test hypotheses regarding the patterns of morphological diversification within Pelobatoidea, forty-six pelobatoid species (n = 960) were used, which was the maximum overlap between morphological and molecular datasets. From this dataset, we measured on average 20 individuals per species (range = 1–111). To test hypotheses regarding the adaptive radiation of megophryid frogs, a separate dataset including just megophryid frogs were also compiled. For this dataset, a total of forty species (n = 812) were used in diversification analyses. From this smaller dataset, we measured on average 21 individuals per species (range = 1–111). All measurements were log transformed to account for non-normality in sampling. All

diversification statistics were performed using source code implemented in R (R Development Core Team, 2006).

First, to capture the variance associated with all morphological measurements a principle components analysis (PCA) was run, and the first several components that explain up to 95% of the variation were extracted. These components were used to examine how morphological variation was partitioned across the phylogeny. To do this, relative disparity (pairwise Euclidean distance between species) was calculated for each subclade of the tree and standardized by dividing the entire tree disparity. Subclades with values near 0 indicate that relatively little variation is present within that clade, while values near 1 indicate that subclades contain much of the total variation (Harmon et al., 2003). To calculate an expected null distribution, we simulated character evolution along the topology under a Brownian motion model of evolution. A distribution of simulated disparities was then calculated. The observed relative morphological disparity was then plotted as a function of time (disparity-through-time plots) and compared to the null distribution. Comparing the area under the curve for the observed and expected disparity assesses the level of significance.

To examine how morphology is evolving across the tree, we fit four models of character evolution to each trait and calculated the fit of the model using AICc scores (AIC corrected for small sample size). The lower the AICc score the better the model fits the data , but for an AICc score to fit significantly better than another the difference must be >4 (Akaike, 1974; Burnham and Anderson, 2002; Burnham and Anderson, 2004). Likelihood modeling was performed using the Geiger package in R (Harmon et al., 2008). The first model explored was Brownian motion (BM), which has a single rate parameter (σ^2) throughout the tree. This model essentially

describes a continuous character randomly walking through time, and estimates expected variation. The second model explored was the early burst model (EB; Blomberg et al., 2003), in which σ^2 decreases with increasing time. This model tests for signature of increased (or burst) variation early in the tree and decreased variance in more recent branches, both of which are expected for adaptively radiating clades. Finally, we tested the fit of the Ornstein-Uhlenbeck process (OU), a random walk model with selective constraints. These two models are similar in that they both model a situation where species maintain central values for their continuous characters (where α measures the strength of selection). The OU model is interesting when intermediate α is detected. A high value for α indicates that strong selection is acting on that character, whereas a lower value for α indicates that selection is less forceful. When $\alpha = 0$ the OU model reduces to the BM model (Butler and King, 2004), and as α approaches ∞ the model is equivalent to white noise (Hunt, 2006).

RESULTS

Topological estimate and divergence times

The consensus tree topology was constructed using maximum clade credibility from all post burn-in trees (160 million). Although the two runs had visually converged in Tracer, the ESS for several parameters did not reach over 200 as expected under convergence.

The resultant topology is largely congruent with other molecular phylogenetic analyses (Frost et al., 2006; Roelants et al., 2007; Wiens, 2007; Figure 1), although we find some

important differences deep in the tree. Support within families is generally high and most form monophyletic groups. However the relationships among families in some cases are different than expected and support at these nodes is weak. For example, the family Megophryidae does not form a sister relationship with the *Pelobates*. Instead *Pelobates*, *Pelodytes*, and the family Scaphiopodidae form a monophyletic group.

It is suggested the family Megophryidae contains eleven genera that form two subfamilies (Megophryinae with five genera and Leptobrachiinae with six genera) based on their two distinct types of larvae and the arrangement of tubercles on the adult hand (Dubois, 1980). Our molecular analysis strongly supports this hypothesis with 100% posterior probability and each proposed genus nested within the correct subfamily (Figure 1). The only exception is the placement of Leptolalax lateralis within the Megophryiinae subfamily. However this species has a long history of taxonomic unstability as it has been proposed to belong to Megophrys (Liu, 1950; Dubois, 1980; Dubois and Ohler, 1998), Xenophrys (Khonsue and Thirakhupt, 2001), and most recently Leptolalax (Delorme et al., 2006). Our results suggest it belongs within the genus Xenophrys.

One of the most interesting results of this study is the discovery of several megophryid genera that are paraphyletic or polyphyletic. Within the subfamily Leptobrachiinae, the genus *Leptolalax* (as described above) is not only paraphyletic with regard to the placement of *L. lateralis*, but also *L. oshanensis* is found within the genus *Leptobrachium*. The genus *Leptobrachium* is further divided by the presence of the genus *Oreolalax*, although this was not recovered by previous studies and has low support in our tree (Brown et al., 2009*)*. Within the subfamily Megophryinae, the genus *Xenophrys* is split between two monophyletic groups that

are not immediate sister clades. The genus *Vibrisapphora* is represented by just one species in our study and may form a monophyletic group, however it is nested within the genus *Brachytarsophrys*. Surprisingly the genus *Megophrys*, which has traditionally been a catch-all genus for unknown megophryids, was found to be monophyletic.

Divergence time estimates indicate older appearances of clades than previously described. Our chronogram suggests a Late Jurassic—Triassic origin of the crown group Pelobatoidea (~200 MY; Figure 1). For the crown group Megophryidae we recover an Early Cretaceous origin (~127 MY), and the origin of its subfamilies Leptobrachiinae in the Late Cretaceous (~85 MY) and Megophryinae in the Paleogene (~56 MY).

Lineage accumulation

The MCCR test revealed a positive gamma statistic ($\gamma = 0.25$; $p = 0.99$) for both the superfamily Pelobatoidea and the family Megophryidae, indicating that there has been no slowing of lineage accumulation through time. Lineage-through-time (LTT) plots suggested that lineages were slow to accumulate early in pelobatoid history (Figure 2A). Furthermore, lineages accumulate in a constant manner across the tree; although there is a small peak that marks the appearance of the family Megphryidae (Figure 2A). When lineage-through-time plots were run for just the megophryid clade, we saw no increased speciation early in the tree that would be expected under an adaptive radiation (Figure 2B). When the effect of missing taxa was incorporated into the simulations and a null distribution was collected, the observed value was in the expected range for lineage accumulation throughout the megophryid tree ($p = 0.35$; Figure 2C).

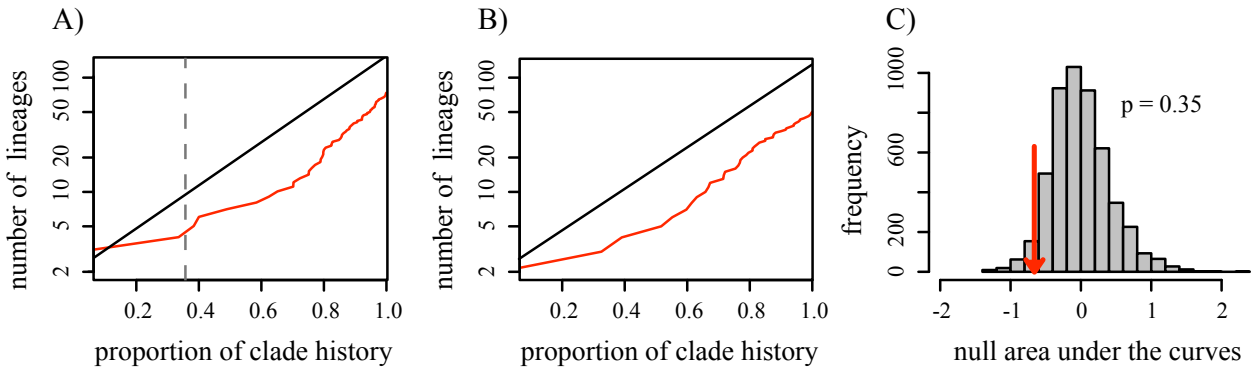

Figure 2. Lineage-through-time plot of (A) pelobatoid frogs and (B) megophryid frogs. Black line indicates pure-birth expectation, red line indicates observed lineages through time. Dashed line indicates megophryid appearance. C) To test whether megophryids have unexpectedly high lineage diversification, we created a null distribution of areas under the curve for 5000 simulations that incorporated missing taxa. Red arrow indicates placement of observed area under the curve.

Morphological diversification

Principle components analysis revealed three components that explain 95% of the variation in the pelobatoid morphological dataset (Table 1). These three components were used for morphological disparity analyses individually and combined. All three components had the strongest loadings from limb lengths and SVL.

Average subclade disparity for combined morphology (first three principle components) remained relatively high throughout early pelobatoid history (Figure 3A). Throughout the majority of pelobatoid history, their relative disparity was within the 95% Brownian motion expectation, however there was a burst of morphological disparity about 75% through the tree (~50 MYA) that showed higher than expected variation (Figure 3A). When this was compared to our null expectation, pelobatoid disparity to be significantly higher than expected ($p = 0.03$; Figure 3B). The relative disparity plots for the family Megophryidae are similar to the relative disparity plots from the superfamily as a whole (Figure 3C). Because these are nested, this indicates that much of the disparity found within Pelobatoidea stems from the disparity found within the family Megophryidae. When megophryid disparity was compared to the null expectation, it was also significant ($p = 0.04$; Figure 3D). Average subclade disparity for the individual components revealed a similar pattern as combined data (Figure 4), but with some marked differences. In general, all three components for both Pelobatoidea and Megophryidae are higher than expected in the last third of the tree. This pattern indicates strong convergence of traits among younger subclades of the tree. However, the components are behaving differently in their degree of disparity. Component 1 is the only component to be higher than the mean expectation for the first two-thirds of the tree, whereas components 2–3 stay close to the mean

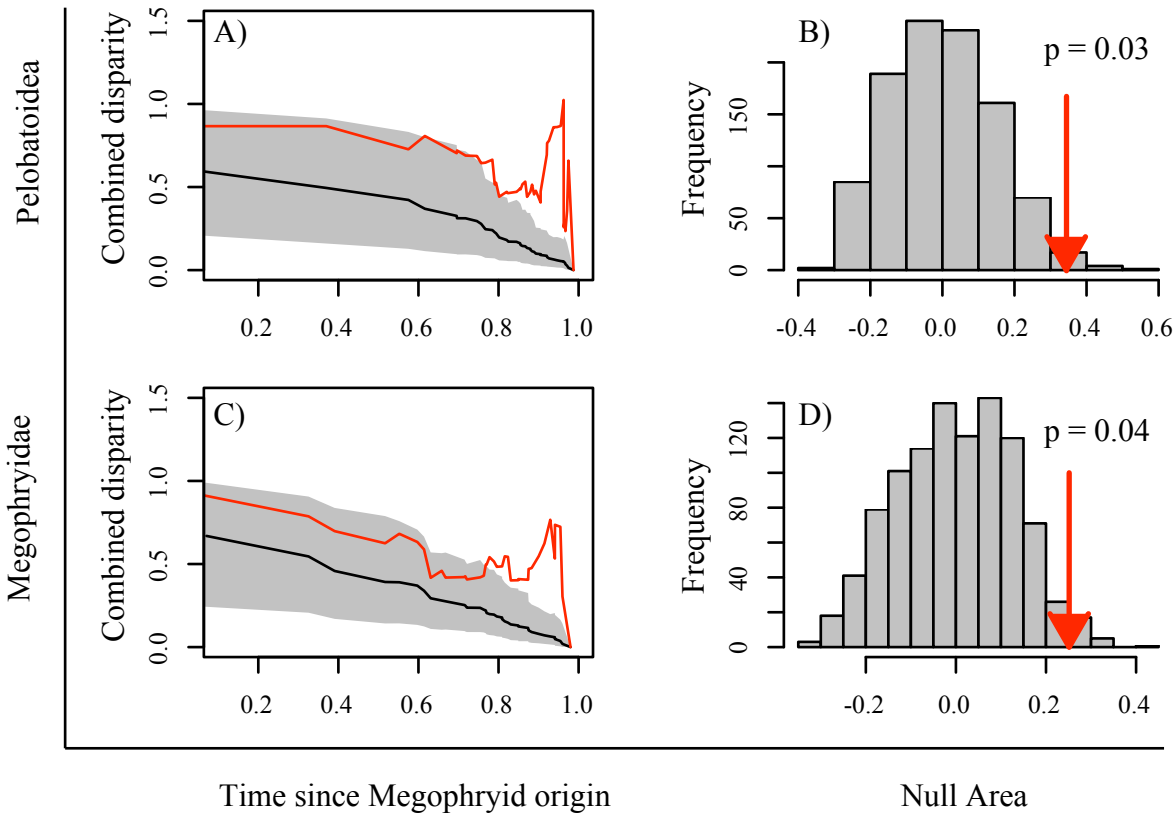

Figure 3. Disparity-through-time plots for combined morphology for the superfamily Pelobatoidea (A; upper) and the family Megophryidae (B; lower). Average disparity is calculated by averaging all ancestral subclades that were present at that given time relative to whole-tree disparity. Time is expressed throughout as proportion of the clade's history (x-axis) that corresponds with Figure 1. Average subclade disparity (red lines) for each point in time is compared with expected disparity based on Brownian morion simulations (black line indicates mean, 95% confidence limit in shaded areas). Null distribution was built from 1000 simulations of areas under the curve and compared to the observed area under the curve for Pelobatoidea (C) and Megophyridae (D).

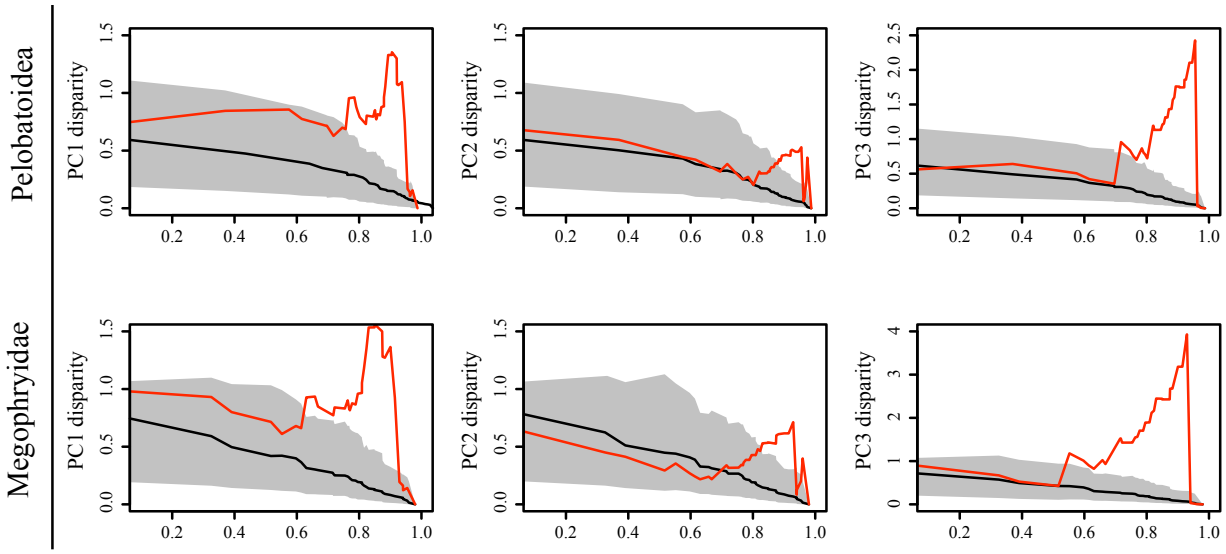

Figure 4. Disparity-through-time plots of individual principle components (PC1–PC3) for the superfamily Pelobatoidea (Upper) and the family Megophryidae (Lower). Average disparity is calculated by averaging all ancestral subclades that were present at that given time relative to whole-tree disparity. Time is expressed throughout as proportion of the clade's history (x-axis) that corresponds with Figure 1. Average subclade disparity (red lines) for each point in time is compared with expected disparity besed on Brownian morion simulations (black line indicates mean, 95% confidence limit in shaded areas).

expectation throughout their first two-thirds of the tree. Despite the similar patterns between Pelobatoidea and Megophryidae, the relative disparity found within Megophryidae is much higher than can be found in Pelobatoidea.

The results from the likelihood models fitting suggest that all traits within Pelobatoidea and Megophryidae are evolving with selective constraints (Ornstein-Uhlenbeck; Table 2). No traits were best fit with Brownian motion, an unbounded random walk, nor the early burst model, which is the pattern expected under adaptively radiating clades.

Table 1. Importance of individual components of pelobatoid morphological data that explain up to 95% of the variation found in the dataset.

Importance of Components	PC1	PC2	PC3
Standard Deviation	0.48	0.15	0.13
Proportion of Variance	0.81	0.08	0.06
Cumulative Proportion	0.81	0.89	0.95

Table 2. AICc scores from likelihood modeling of four models of evolution: Brownian motion (BM), Ornstein-Uhlenbeck (OU), and early burst (EB); the best fit model is bolded. All values were log transformed. Snout-vent length (SVL), pelvic width (PlW), pectoral width (PcW), head length (HeL), head width (HeW), intraoccular distance (ID), eye height (EH), ilium length (IL), femur length (FeL), tibiafibula length (TL), calcaneous length (CL), foot length (FoL), humoral length (HuL), radioulna length (RL), hand length (HaL)

	Superfamily Pelobatoidea														
	SVL	PlW	PcW	HeL	HeW	ID	EH	IL	FeL	TL	CL	FoL	HuL	RL	HaL
BM	-36	-24	-17	-33	-19	-32	-32	-43	-45	-46	-53	-40	-37	13	-48
OU	**-56**	**-40**	**-37**	**-47**	**-31**	**-43**	**-47**	**-57**	**-63**	**-60**	**-68**	**-60**	**-56**	**-23**	**-65**
EB	-34	-15	-15	-30	-17	-29	-30	-40	-43	-43	-52	-37	-35	16	-45
	Family Megophryidae														
	SVL	PlW	PcW	HeL	HeW	ID	EH	IL	FeL	TL	CL	FoL	HuL	RL	HaL
BM	-26	-16	-11	-23	-11	-22	-25	-32	-34	-34	-40	-29	-26	16	-36
OU	**-43**	**-29**	**-26**	**-33**	**-20**	**-31**	**-37**	**-46**	**-49**	**-46**	**-52**	**-44**	**-43**	**-17**	**-50**
EB	-24	-14	-8	-20	-9	-20	-23	-30	-32	-31	-38	-26	-24	19	-33

DISCUSSION

The development of robust phylogenetic hypotheses is necessary for any analysis of evolutionary events. The phylogeny presented in this study is used for tests of lineage accumulation and morphological diversification, but the evolutionary questions it can be used to address in the future are endless.

Systematics of megophryid frogs

Although our phylogeny shows some topological incongruences in the relationships of megophryid frogs to their sister taxa from other studies, these are likely the result of low ESS values and runs not reaching convergence. We see incongruence at places in our tree where posterior support is low, and therefore more data or more MCMC generations might diminish differences. Given that these occur near the base of the tree, it is unlikely that these results mislead the diversification analyses.

This study is the first large-scale investigation into megophryid relationships, however this is not the first study to cast doubt on the monophyly of traditionally recognized megophryid groups (Lathrop, 1997; Xie and Wang, 2000; Delorme and Dubois, 2001; Frost et al., 2006; Zheng et al., 2008). The discordance we find within each subfamily of megophryids is a result of the disarranged taxonomy of megophryids. The family has a long history of naming and cataloging species in the absence of a molecular phylogeny, thus many (if not most) species come with a long list of synonyms. Although megophryid systematists tend to agree upon ten genera for the group, this seems to be mostly based on morphological classification rather than

monophyloetic groupings. The results from our study indicate that several of these groups are not natural and will need to be re-categorized based on new molecular evidence.

Evolutionary diversification of Pelobatoidea

The results from our lineage accumulation analyses show that pelobatoids have had a constant rate of growth since their origin. We do not see evidence of a slow down either (as shown with the MCCR test). If the MCCR test was a two-tailed test, it might even indicate that rate of lineage accumulation has increased in recent pelobatoid history. Unfortunately, the MCCR has no power to test rate increases due to extinction and the pull of the present (Pybus and Harvey, 2000). Other rate shift tests could be beneficial to use within the group, such as MEDUSA (Modeling Evolutionary Diversification Using Stepwise AIC; Alfaro et al., 2009a), which tests for branches leading to exceptional or depauperate species richness. This method integrates the timing of early splits in the tree with taxonomic richness data and produces ML estimates of speciation and extinction. The model estimates speciation and extinction for subclades as well, and evaluates if they significantly depart from whole-tree estimates (indicating a speed-up or slow-down diversification rate). Although this is the type of analysis needed to answer some of the more interesting questions regarding the evolution of this group, the taxonomic uncertainty and questionable monophyly found within the family Megphryidae would cause problems at this stage.

Our morphological analyses suggest that pelobatoid traits are not evolving under a Brownian motion model of evolution. For all 15 traits the Ornstein-Uhlenbeck model, a random walk with a selective constraint, significantly improved the fit of the data indicating that traits are

returning to central values (all ΔAICc > 4; Table 2). The disparity results bolster this evidence further, showing that young clades have significantly higher variances than expected under a Brownian motion model (Figures 2 and 3).

Morphological diversity within Pelobatoidea has remained relatively high throughout their history, however within the last 40 MY pelobatoids have increased variation considerably. It is likely that the majority of variation found within Pelobatoidea is due to variation found within the Family Megophryidae, as the megophryid clade shares the same pattern of disparity at a higher scale (Figures 2–3). Within pelobatoid subclades, relative disparity is high, and members of these clades are morphologically distinct. However, between subclades diversity is lower, indicating that subclades contain relatively the same amount of diversity. This indicates that pelobatoid subclades initially diversified into different ecological clines, and within the last 40 MY subclades have repeatedly converged into similar niches.

Have Megophryids undergone an adaptive radiation?

Morphological diversification and speciation are of fundamental interest to evolutionary biologists because they are the generators of biodiversity. Although studies of diversity may focus largely on one component or the other, there are some recognized phenomena that should link them. One of these is adaptive radiation, which is thought to lead to increased rates in both trait variability and species diversity (Schluter, 2000; Gavrilets and Losos, 2009). Many radiations are described qualitatively, which is problematic as recent evidence suggests some of the classic radiations might not have exceptional diversity after all (Alfaro et al., 2009a)

For the family Megophryidae, despite their large clade size and high degree of variation, we do not see the classic signature of adaptive radiation. Lineage-through-time plots show no burst in speciation, nor do we see a slow down of rates with the MCCR test, both of which are expected under burst speciation. Furthermore, evidence for morphology shows that the most variation is found near the tips (within subclades), indicating recent morphological expansion. These data suggest that some other mechanism (perhaps iterative adaptive radiations or niche-filling models) is responsible for the morphological diversity seen in megophryids.

LITERATURE CITED

Akaike, H. 1974. A new look at the statistical model identification. IEEE Trans. Automat. Contrl. 19:716–723.

Alfaro, M. E., F. Santini, C. Brock, H. Alamillo, A. Dornburg, D. L. Rabosky, G. Carnevale, and L. J. Harmon. 2009a. Nine exceptional radiations plus high turnover explain species diversity in jawed vertebrates. Proceedings of the National Academy of Sciences 106(32): 13410–13415.

Alfaro, M. E., D. R. Karns, H. K. Voris, and B. L. Stuart. 2008. Phylogeny, evolutionary history, and biogeography of oriental-australian rear-fanged water snakes (Colubridae: Homalopsidae) Inferred from Mitochondrial and Nuclear DNA Sequences. Molecular Phylogenetics and Evolution 46(2):576–593.

Alfaro, M. E., F. Santini, and C. D. Brock. 2007. Do reefs drive diversification in marine teleosts? Evidence from the pufferfishes and their allies (Order Tetraodontiformes) Evolution 61(9):2104–2126.

Blomberg S. P., T. Garland, and A. R. Ives. 2003. Testing for phylogenetic signal in comparative data: Behavioral traits are more labile. Evolution 57(4):717–745.

Brown, R. M., C. D. Siler, A. C. Diesmos, and A. C. Alcala. 2009. Philippine frogs of the genus *Leptobrachium* (Anura; Megophryidae): Phylogeny-based species delimitation, taxonomic review, and descriptions of three new species. Herpetological Monographs 23:1–44.

Burnham, K. P., and D. R. Anderson. 2004. Multimodel inference—understanding AIC and BIC in model selection. Sociological methods and research 33(2):261–304.

Burnham, K. P., and D. R. Anderson. 2002. Model selection and multimodel inference: a practical information-theoretic approach. 2nd Edition. Springer-Verlag, New York, New York, USA. 488 pp.

Butler, M. A., and A. A. King. 2004. Phylogenetic comparative analysis: a modeling approach for adaptive evolution. American Naturalist 164:683–695.

Delorme, M., A. Dubois, S. Grosjean and A. Ohler. 2006. Une nouvelle ergotaxinomie des Megophryidae (Amphibia, Anura). Alytes. 24(1–4):6–21.

Delorme, M., and A. Dubois. 2001. Une nouvelle espèce de Scutiger du Bhutan, et quelques remarques sur la classification subgénérique du genre Scutiger (Megophryidae, Leptobrachiinae). Alytes 19:141–153.

Drummond, A. J., and A. Rambaut. 2003. BEAST v1.0. http://evolve.zoo.ox.ac.uk/beast/.

Drummond, A. J., S. Y. W. Ho, M. J. Phillips, and A. Rambaut. 2006. Relaxed Phylogenetics and Dating with Confidence. PLoS Biology 4:699–710.

Dubois, A. 1980. Notes sur la systematique et la repartition des amphibiens anoures de Chine et des regions avoisinantes IV. Classification generique et subgenerique des Pelobatidae Megophryinae. Bulletin Mensuel de la Société Linnénne de Lyon 49: 469–482.

Dubois, A., and A. Ohler. 1998. A new species of *Leptobrachium* (*Vibrissaphora*) from northern Vietnam, with a review of the taxonomy of the genus *Leptobrachium* (Pelobatidae, Megophyinae). Dumerilia 4: 1–32.

Dubois, A. 2005. Amphibia Mundi. 1.1. An ergotaxonomy of Recent amphibians. Alytes 23:1–24.

Edgar, R. C. 2004. MUSCLE: a multiple sequence alignment method with reduced time and space complexity. BMC Bioinformatics 5:113.

Frost, D. R., T. Grant, J. Faivovich, R. H. Bain, A. Haas, C. F. B. Haddad, R. O. De Sa, A. Channing, M. Wilkinson, S. C. Donnellan, C. J. Raxworthy, J. A. Campbell, B. L. Blotto, P. Moler, R. C. Drewes, R. A. Nussbaum, J. D. Lynch, D. M. Green, W. C. Wheeler. 2006. The amphibian tree of life. Bulletin of the AMNH (no. 297) 370 p.

Gavrilets, S., and J. B. Losos. 2009. Adaptive radiation: contrasting theory with data. Science 323:732–736.

Garcia-Paris, M., D. R. Buchholz, and G. Parra-Olea. 2003. Phylogenetic relationships of Pelobatoidea re-examined using mtDNA. Molecular Phylogenetics and Evolution 28:12–23.

Gittenberger, E. 1991. What about non-adaptive radiation? Biological Journal of the Linnean Society 43:263–272.

Graybeal, A. 1997. Phylogenetic relationships of bufonid frogs and tests of alternate macroevolutionary hypotheses characterizing their radiation. Zoological Journal of the Linnean Society. London 119:297–338.

Harmon, L. J., J. Melville, A. Larson, and J. B. Losos. 2008. The Role of Geography and Ecological Opportunity in the Diversification of Day Geckos (Phelsuma). Systematic Biology 57:562–573.

Harmon, L. J. , J. A. Schulte II, A. Larson, J. B. Losos. 2003. Tempo and Mode of Evolutionary Radiation in Iguanian Lizards. Science 301:961–964.

Henrici, A.C. 2000. Reassessment of the North American pelobatid anuran *Eopelobates guthriei*. Annals Carnegie Museum 69:145–156.

Hunt, G. 2006. Fitting and comparing models of phyletic evolution: random walks and beyond. Paleobiology 32:578–601.

Khonsue, W. and K. Thirakhupt. 2001. A checklist of the amphibians in Thailand. The Natural History Journal of Chulalongkorn University 1(1):69–82.

Kozak, K. H., D. W. Weisrock, and A. Larson. 2006. Rapid lineage accumulation in a non-adaptive radiation: phylogenetic analysis of diversification rates in eastern North American woodland salamanders (Plethodontidae : Plethodon). PROC Biological Sciences Series 273(1586):539–546.

Lathrop, A. 1997. Taxonomic review of the megophryid frogs (Anura: Pelobatoidea). Asiatic Herpetological Research 7:68–79.

Liu, C.-C. 1950. Amphibians of western China. Fieldiana. Zoology Memoires 2: 1–397 + 10 pl.

Losos, J. B., and D. B. Miles. 2002. Testing the Hypothesis That a Clade Has Adaptively Radiated: Iguanid Lizard Clades as a Case Study. The American Naturalist 160(2):147–157.

Lovette, I. J., E. Bermingham, and R. E. Ricklefs. 2002. Clade-specific morphological diversification and adaptive radiation in Hawaiian songbirds. Proceedings of the Royal Society of London B, Biological Sciences 269:37–42.

Mangel, M., H. K. Kindsvater, M. B. Bonsall. 2007. Evolutionary analysis of life span, competition, and adaptive radiation, motivated by the Pacific rockfishes (Sebastes). Evolution 61(5):1208–1224.

Nee, S., A. O. Mooers, and P. H. Harvey. 1992. Tempo and mode of evolution revealed from molecular phylogenies. Proc. Natl. Acad. Sci. 89:8322–8326.

Nosil, P., and B. J. Crespi. 2006. Experimental evidence that predation promotes divergence in adaptive radiation. Proceedings of the National Academy of Sciences 103(24):9090–9095.

Pybus, O. G., and P. H. Harvey. 2000. Testing macro-evolutionary models using incomplete molecular phylogenies. Proceedings of the Royal Society of London Series B-Biological Sciences 267:2267–2272.

Rambaut, A., 1996. Se-Al sequence alignment editor University of Oxford, http://evolve.zoo.ox.ac.uk/software/Se-Al, Oxford, U.K.

Rambaut, A., and A. J. Drummond. 2007. Tracer v1.4, Available from http://beast.bio.ed.ac.uk/Tracer.

Rannala, B., and Z. Yang. 2007. Inferring speciation times under an episodic molecular clock. Systematic Biology 56:453–466.

Roelants, K., D. J. Gower, M. Wilkinson, S. P. Loader, S. D. Biju, K. Guillaume, L. Moriau, and F. Bossuyt. 2007. Global patterns of diversification in the history of modern amphibians. PNAS 104 (3):887–892.

Schluter, D. 2000. The ecology of adaptive radiation. Oxford University Press, Oxford.

Trueb, L., and A. M. Báez. 2006. Revision of the early Cretaceous *Cordicephalus* from Israel and an assessment of its relationships among pipoid frogs. Journal of Vertebrate Paleontology 26(1):44–59.

Webb, J. K., and R. Shine. 1994. Feeding habits and reproductive biology of Australian pygopodid lizards of the genus Aprasia. Copeia 1994:390–398.

Wiens, J. J. 2007. Global Patterns of Diversification and Species Richness in Amphibians. American Naturalist 170(2)86–106.

Wilgenbusch, J. C., D. L. Warren, and D. L. Swofford. 2004. AWTY: A system for graphical exploration of MCMC convergence in Bayesian phylogenetic inference. http://ceb.csit.fsu.edu/awty.

Xie, F., and Z. Wang. 2000. Review of the systematics of pelobatids. Cultum Herpetologica Sinica 8: 356–370. [In Chinese.]

Yang, Z., and B. Rannala 2006. Bayesian estimation of species divergence times under a molecular clock using multiple fossil calibrations with soft bounds. Mol Biol Evol 23:212–226.

Zheng, Y., L. Shuqiang, and J. Fu. 2008. A phylogenetic analysis of the frog genera *Vibrissaphora* and *Leptobrachium*, and the correlated evolution of nuptial spine and reversed sexual size dimorphism. Molecular Phylogenetics and Evolution 46(2):695–707.